

2016

Effects of Synthetic Ligands on Heterodimer Pairs Regarding Full-Length Human PPAR α , RXR α and LXR α

Emily Delman
Wright State University

Follow this and additional works at: https://corescholar.libraries.wright.edu/etd_all



Part of the [Molecular Biology Commons](#)

Repository Citation

Delman, Emily, "Effects of Synthetic Ligands on Heterodimer Pairs Regarding Full-Length Human PPAR α , RXR α and LXR α " (2016). *Browse all Theses and Dissertations*. 1560.
https://corescholar.libraries.wright.edu/etd_all/1560

This Thesis is brought to you for free and open access by the Theses and Dissertations at CORE Scholar. It has been accepted for inclusion in Browse all Theses and Dissertations by an authorized administrator of CORE Scholar. For more information, please contact library-corescholar@wright.edu.

EFFECTS OF SYNTHETIC LIGANDS ON HETERODIMER PAIRS REGARDING
FULL-LENGTH HUMAN PPAR α , RXR α AND LXR α

A thesis submitted in partial fulfillment
of the requirements for the degree of
Master of Science

By

EMILY DELMAN

B.S. Chemistry, Wright State University, 2014

2016

Wright State University

WRIGHT STATE UNIVERSITY

GRADUATE SCHOOL

July, 2016

I HEREBY RECOMMEND THAT THE THESIS PREPARED UNDER MY SUPERVISION BY Emily Delman ENTITLED Effects of Synthetic Ligands on Heterodimer Pairs Regarding Full-Length Human PPAR α , RXR α and LXR α BE ACCEPTED IN PARTIAL FULFILLMENT OF THE REQUIREMENTS FOR THE DEGREE OF Master of Science.

S. Dean Rider, Jr., Ph.D.
Thesis Director

Madhavi P. Kadakia, Ph.D.
Department Chair

Committee on
Final Examination

S. Dean Rider, Jr., Ph.D.

Lawrence J. Prochaska, Ph.D.

Weiwen Long, Ph.D.

Steven J. Berberich, Ph.D.

Robert E.W. Fyffe, Ph.D.
Vice President for Research and
Dean of the Graduate School

ABSTRACT

Delman, Emily. M.S., Department of Biochemistry and Molecular Biology, Wright State University, 2016. Effects of Synthetic Ligands on Heterodimer Pairs Regarding Full-Length Human PPAR α , RXR α and LXR α .

Nuclear receptor study is critically relevant in therapeutic medicine since the intricate details of disease states pertaining to atherosclerosis and diabetes are poorly understood. Three nuclear receptors of interest regulate target genes pertaining to cholesterol and fatty acid regulation, linking these receptors to therapeutic medicine. The first is the peroxisome proliferator-activated receptor alpha (PPAR α), which resides in liver and muscle, coordinating lipoprotein and fatty acid homeostasis [1]. Cholesterol homeostasis is dictated by the liver X receptor alpha (LXR α), targeting genes pertaining to the kidney, intestine, liver and adipose tissues [2]. A common partner receptor to PPAR α and LXR α is known as the retinoid X receptor alpha (RXR α) [3]. Although each receptor appears unique in function, the cause and effects of disease states are poorly understood due to the promiscuous nature of these receptor proteins. These particular receptors can form permissive heterodimers where metabolic effects can be manipulated by ligands [3]. Accordingly, clinical care becomes increasingly complex as synthetic ligands made to target one receptor could have additional repercussions. With respect to therapeutic medicine, ligand binding may not be exclusive. Therefore, it becomes necessary to study synthetic ligands with each receptor, individually and in heterodimeric form, to further understand the complex regulation and clinical implications of synthetic ligands on disease states such as atherosclerosis and diabetes.

TABLE OF CONTENTS

	Page
I. INTRODUCTION.....	1-20
• PPAR.....	2
• LXR.....	4
• RXR.....	6
• Heterodimers.....	8
• Cross Talk.....	10
• Ligand-Binding Domain.....	11
• Natural and Synthetic Ligands.....	12
II. HYPOTHESIS AND AIMS.....	21
III. MATERIALS AND METHODS.....	22-43
• Plasmid Construction for hPPAR α , hLXR α and hRXR α	22-24
• Recombinant Protein Purification.....	25-27
i. Protein Expression in Escherichia.coli.....	25
ii. Purification via Affinity Chromatography.....	25
iii. Protein Concentration and Purity.....	26
• Protein-Protein Interactions in vitro.....	28-34
i. Ligand-Binding Assays.....	28
ii. Circular Dichroism (CD)	29

iii.	Fluorescence Resonance Energy Transfer (FRET)	32
•	Protein-Protein Interactions <i>in vivo</i>	35-43
i.	COS-7 Stable Transfection.....	37
ii.	DNA Isolation.....	39
iii.	Polymerase Chain Reaction.....	39
iv.	COS-7 Transient Transfections.....	40
v.	Fluorescence Microscopy.....	43
IV.	RESULTS.....	44-72
•	SDS-PAGE analysis showed the presence of a 50kDa protein, corresponding to full-length, recombinant proteins used in sequential experiments.....	44
•	Intrinsic fluorescence quenching assays demonstrate ligand binding is not exclusive.....	46
•	Synthetic Ligands induce changes in the secondary structure of the hPPAR α -hLXR α heterodimer.....	51
•	Alexa Fluor dyes 488 and 555 are optimal for fluorescence resonance energy transfer (FRET) experiments.....	55
•	Nuclear receptors hPPAR α and hLXR α bind with high affinity, as shown by FRET.....	60
•	Synthetic ligands have an effect on the binding affinity of hLXR α and hPPAR α	62
•	Stably transfected COS-7 cells contain all three nuclear receptor plasmids, as shown with PCR testing.....	65

- BiFC quantitative analysis indicates variation in subcellular localization of transiently transfected COS-7 cells, in response to synthetic ligands..... 67

V. DISCUSSION.....	73-80
VI. LIST OF ABBREVIATIONS.....	81-82
VII. REFERENCES.....	83-87
VIII. APPENDIX.....	88-92

LIST OF FIGURES

Figure	Page
1. Synthetic compounds and their corresponding structures.....	15
2. Primers used for amplification from cDNA derived from HepG2 cells	
(A) hPPAR α	22
(B) hLXR α	22
(C) hRXR α	22
3. Schematic of plasmid DNA constructs for full-length His-tagged proteins	
(A) hLXR α	24
(B) hPPAR α	24
(C) hRXR α	24
4. Schematic of BiFC constructs where hPPAR α is the central protein...	36

5. Schematic of plasmid DNA construction for bimolecular fluorescence complementation using stable transfections	
(A) VenusN172-LXR α	38
(B) CeruleanN172-RXR.....	38
(C) ECFPC155-PPAR α	38
6. Schematic of plasmid DNA construction for bimolecular fluorescence complementation using transient transfections	
(A) VenusN172-hPPAR α	42
(B) ECFPC155-hLXR α	42
7. SDS-PAGE showing purified, full-length hPPARα, hRXRα and hLXRα	
(A) hPPAR α	45
(B) hRXR α	45
(C) hLXR α	45

8. Intrinsic fluorescence quenching of hLXRα, hPPARα and hRXRα with synthetic ligands used in further assays	
(A-C) Auraptene.....	48
(D-F) UVI-3003.....	48
(G-I) Pravastatin.....	48
(J-L) GW-6471.....	48
(M-O) Lovastatin.....	48
9. Intrinsic fluorescence quenching of hLXRα, hPPARα and hRXRα with synthetic ligands used in further assays	
(A-C) Ciprofibrate.....	49
(D-F) Fluorobexarotene.....	49
(G-I) T-0901317.....	49
10. Circular Dichroic spectra of a mixture of hPPARα and hLXRα in the presence and absence of synthetic ligands	
(A) Fluorobexarotene.....	53
(B) Ciprofibrate.....	53
(C) T-0901317.....	53

11. Fluorescent binding assays using Alexa Fluor (AF) 555-labeled

protein, titrated against increasing concentrations of unlabeled protein

(A) AF-555hPPAR α + hRXR α	57
(B) AF-555hPPAR α + hLXR α	57
(C) AF-555hRXR α + hLXR α	57
(D) AF-555hRXR α + hPPAR α	57

12. Fluorescent binding assays using Alexa Fluor (AF) 488-labeled

protein, titrated against increasing concentrations of unlabeled protein

(A) AF-488hLXR α + hRXR α	58
(B) AF-488hLXR α + hPPAR α	58
(C) AF488hPPAR α + hRXR α	58
(D) AF-488hPPAR α + hLXR α	58
(E) AF-488hRXR α + hLXR α	58
(F) AF-488hRXR α + hPPAR α	58

13. Fluorescent binding assays using Alexa Fluor (AF) 594-labeled

protein, titrated against increasing concentrations of unlabeled protein

(A) AF-594hRXR α + hLXR α	59
(B) AF-594hRXR α + hPPAR α	59

14. FRET using AF-488hLXRα as the donor and AF-555hPPARα	
as the acceptor	
(A) FRET spectra.....	61
(B) Binding curve.....	61
15. FRET using AF-488hLXRα as the donor and AF-555hPPARα	
as the acceptor in the presence of synthetic ligands	
(A) Ciprofibrate.....	63
(B) T-0901317.....	63
(C) Fluorobexarotene.....	63
16. Electrophoresis showing the presence of nuclear receptor	
plasmids in COS-7 stably transfected cells	
(A) hLXR α	66
(B) hPPAR α	66
(C) hRXR α	66
17. Fluorescence microscopy of stably transfected COS-7 cells	
in the absence of ligand	
(A) CFP.....	70
(B) YFP.....	70
(C) Overlay.....	70
(D) DIC + Overlay.....	70

18. Fluorescence microscopy indicates nuclear fluorescence for all transiently transfected COS-7 cells, in the absence and presence of synthetic ligand	
(A-B) Wild Type.....	71
(C-D) Fluorobexarotene.....	71
(E-F) Ciprofibrate.....	71
(H-I) T-0901317.....	71
19. Quantitative analysis of transiently transfected COS-7 cells in response to synthetic ligands where ECFP-hPPARα is the central partner receptor	
(A) Fluorescence Intensity.....	72
(B) Co-localization.....	72

APPENDIX

1. Circular Dichroic spectra of a mixture of hPPARα and hLXRα in the presence and absence of synthetic ligands	
(A) Auraptene.....	90
(B) GW-6471.....	90
2. FRET using AF-488hLXRα as the donor and AF-555hRXRα as the acceptor	
(A) FRET spectra.....	91
(B) Binding curve.....	91
3. Quantitative analysis of transiently transfected COS-7 cells in response to synthetic ligands where ECFP-hPPARα is the central partner receptor	
(A) Fluorescence Intensity.....	92
(B) Co-localization.....	92
4. Quantitative analysis of transiently transfected COS-7 cells in response to synthetic ligands where ECFP-hLXRα is the central partner receptor	
(A) Fluorescence Intensity.....	93
(B) Co-localization.....	93

LIST OF TABLES

Table	Page
1. Composition of high salt PBS buffer.....	34
2. Intrinsic fluorescence quenching of 100nM hLXR α , hPPAR α and hRXR α titrated with synthetic ligands (100 μ M).....	50
3. Secondary structures of hPPAR α and hLXR α (corrected for solvent effect) in the presence and absence of synthetic ligands.....	54
4. Fluorescence resonance energy transfer of 25nM AF-488hLXR α titrated against AF-555hPPAR α over a range of 0nM to 100nM in the presence and absence of synthetic ligands.....	64

APPENDIX

1. Intrinsic fluorescence quenching of 100nM hLXR α , hPPAR α and hRXR α titrated with synthetic ligands (100 μ M)..... 89
2. Secondary structures of hPPAR α and hLXR α (corrected for solvent effect) in the presence and absence of synthetic ligands..... 90

ACKNOWLEDGEMENTS

I would like to thank the late Dr. Heather Hostetler for the opportunity to be a part of her lab. Her patience, kindness and dedication to research served as an example to all graduate students. The passion and commitment she had for teaching others allowed me to complete this thesis project, even in her absence. I would also like to thank Dr. Dean Rider for stepping in and continuing her legacy. The completion of this project would not have been possible without Dr. Rider's guidance, expertise, and dedication. My committee, Dr. Lawrence Prochaska, Dr. Steven Berberich, Dr. Weiwen Long and Dr. Dean Rider has undeniably remained pillars during a time of many unknowns. I greatly appreciate their support as well as the Wright State University Biochemistry and Molecular Biology department as we continue Dr. Heather Hostetler's initiatives. To all the past and present lab members of the Hostetler lab, thank you for your support and assistance. A special thanks to Shimpi Bedi and Andrea Klingler, for their encouragement and willingness to assist during a challenging time. I would also like to thank my family and friends, especially, Richard, Linda, and Allegra Delman as well as Joshua Imwalle for their patience and encouragement throughout my graduate school experience.

I. INTRODUCTION

Numerous homeostatic biological processes are highly dependent on a class of proteins known as nuclear receptors. These receptors can work together as either heterodimers or homodimers to regulate genes pertaining to metabolism. A general nuclear receptor is composed of a N-terminal domain, DNA binding domain, ligand binding domain and a C-terminal domain. The ligand-binding domain is a key aspect of nuclear receptors since a ligand could induce a change in secondary structure, resulting in transcriptional changes, which would presumably have an effect on metabolism. Genetic regulation is dependent on ligand binding to initiate transcription where ligands include steroid hormones, lipids and other molecules for metabolic regulation. Since nuclear receptor ligands bind with high specificity, a defect in the ligand-binding pocket can cause detrimental effects to the cell where the ligand is unable to bind, thus transcription does not occur for a particular gene. This ligand specificity can be utilized to engineer synthetic ligands, potentially directing a cell to activate or inhibit transcription. Nuclear receptor signaling and dimerization are intrinsically linked and critically relevant to therapeutic medicine. Three nuclear receptor proteins of interest are the peroxisome proliferator-activated receptor alpha ($PPAR\alpha$), liver X receptor alpha ($LXR\alpha$) and retinoid X receptor alpha ($RXR\alpha$), all of which contain transactivation and transrepression functions [2]. Nuclear receptors

play a key role in biological processes, covering a diverse range of diseases and disorders that are a primary focus for study.

Diseases such as atherosclerosis, hypertension, insulin resistance and hypertriglyceridemia stem from metabolic disorders linked to diabetes, often resulting from obesity [2]. Nuclear receptors, such as PPAR α and LXR α , regulate lipid homeostasis and are closely linked to aspects of metabolic function, such as inflammation, driven by macrophages in arterial walls [2]. Accordingly, therapeutic treatment calls for pharmaceutical profiles, which can exclusively target mis-regulated homeostatic pathways, driven by these nuclear receptors.

PPAR

First discovered in the 1990's (Rakhshanderhoo et. al, 2010), the PPAR nuclear receptor has been shown to modulate homeostatic effects pertaining to lipoprotein metabolism and other physiological outcomes related to fatty acid synthesis and regulation [1]. Certain isoforms exist for each receptor protein, for example, there are three subtypes of PPAR including PPAR α , PPAR δ and PPAR γ . Each isoform is known to dimerize with the retinoid X receptor (RXR) to carry out metabolic processes throughout the body. Similarities for the subtypes include natural ligands since all PPAR's tend to bind eicosanoids and fatty acids. However, each isoform exhibits differences in metabolic function depending on tissue specificity.

The alpha isoform of PPAR resides in the liver and muscle, responsible for regulation of glucose metabolism, ketone body synthesis and fatty acid oxidation [4].

Natural ligands such as unsaturated fatty acids bind to PPAR α with high affinity while saturated fatty acids demonstrate lower affinity binding [4]. Additionally, other studies have shown that PPAR α binds to 8-(S)-hydroxyeicosatetraenoic acid, another endogenous ligand, which is linked to inflammatory responses [4]. Natural ligands have characteristically high binding affinities (nanomolar range), therefore a proposed explanation includes a promiscuous ligand-binding pocket, possessing the ability to bind a host of endogenous lipid derivatives [4]. Synthetic ligands are often used to study binding affinities as well, the most commonly studied being fibrate drugs. These drugs are currently used in pharmaceutical approaches to lower triglycerides and raise high-density lipoprotein (HDL) cholesterol levels, providing a beneficial response for patients suffering from hypertriglyceridemia [4].

The PPAR gamma subtype can be found in adipose tissue, liver and muscle, where it is responsible for fat synthesis and storage [4]. By promoting triglyceride storage and adipocyte formation, PPAR γ is intrinsically involved in insulin sensitivity, which is a point of interest for therapeutic drug development [4]. Natural ligands for PPAR γ include unsaturated fatty acids such as eicosapentaenoic acid, arachidonic acid, oleate and linoleate as well as some prostaglandins [4]. Synthetic ligands for this isoform include antidiabetic compounds such as thiazolidinediones (TZD). Lastly, the PPAR delta isoform partakes in thermogenesis and fatty acid oxidation. Although PPAR δ is ubiquitously expressed, it can fulfill PPAR α requirements such as fatty acid oxidation in the absence of PPAR α [4].

Metabolic effects seen by PPAR are dictated by a genetic sequence known as the peroxisome proliferator response element (PPRE). This PPRE is separated by one

nucleotide (direct repeat-DR1) and is known to contain a direct repeat consisting of the sequence, AGGTCA [1]. Additionally, PPAR is responsible for regulating genes such as the fatty acid binding protein 1 (FABP1), peroxisomal acyl-coenzyme A oxidase (ACOX1), apolipoprotein A1 (APOA1), ATP-binding cassette transporter (ABCA1) and others pertaining to lipid metabolism.

This nuclear receptor targets the enzyme, HMG-CoA synthase, aiding in ketone body production [2]. Particularly, the alpha isoform is of significance since it is found in the liver where abnormal regulation results in the chronic diseases associated with obesity and diabetes [5]. With regards to therapeutic treatment, PPAR α has been shown to increase insulin sensitivity in mice, suggesting its regulation could be of potential benefit for diabetic human patients [2]. Effects seen by PPAR α can be manipulated by synthetic ligands, providing metabolic benefits where synthetic ligands targeting PPAR α , have been shown to decrease triglyceride levels and increase HDL's in plasma, leading to clinical treatment for diseases such as hyperlipidemia [1]. Accordingly, PPAR α is an attractive target for therapeutic agents due to its large, hydrophobic ligand-binding pocket (1300-1400 Å) and ability to bind multiple targets, in which a host of synthetic ligands become available [6, 7, 8].

LXR

The liver X receptor (LXR) exists in two isoforms, alpha and beta, which play a role in cholesterol homeostatic pathways by binding oxysterols. The beta isoform is ubiquitous while the alpha isoform shows tissue specificity, exhibiting feedback regulation [2]. Primarily focusing on LXR α , many target genes have been identified,

where protein expression is found in the kidney, intestine, liver and adipose tissue, where mis-regulation results in diseases linked to obesity and diabetes [9]. Among the first genes identified as targets of LXR α regulation was cholesterol 7 α -hydroxylase (CYP7A1), leading to the conclusion that LXR has a regulatory role in bile acid synthesis [9]. Additional genes targeted for LXR α regulation include the sterol regulatory element-binding protein (SREBP-1), ATP binding cassette genes (ABC), lipoprotein lipase (LPL), cholesterol regulatory element binding protein (ChREBP), and apolipoprotein (ApoE), all of which maintain cholesterol homeostasis throughout the human body. Liver X receptor alpha target genes also assist in reverse cholesterol transport, particularly linked to the liver and intestine.

Interestingly, LXR α is known to dimerize with RXR α , binding to two direct repeats (AGGTCA) [9]. Each direct repeat is divided by a four-nucleotide segment (DR4), known as the LXR response element (LXRE) [9]. Additionally, it has recently been shown that LXR α can dimerize with PPAR α as well, however, cellular effects are not well understood. Previously identified natural ligands for LXR α are 24-(S), 25-epoxycholesterol and 22-(R)-hydroxycholesterol, found in the liver and adrenal gland, respectively [9]. Other natural ligands include oxysterols, where the liver X receptor can serve as a “cholesterol sensor” by up-regulating genes to enhance cholesterol transport and catabolism when oxysterol concentrations are elevated [9]. Therefore, detrimental effects seen with high cholesterol could be regulated by target genes activated through LXR α , linking this nuclear receptor to cholesterol metabolism.

Regarding diseases, such as atherosclerosis, it has been shown that genetic influence can have beneficial effects on metabolic regulation. For example, a study using hypercholesterolemic mice demonstrated a beneficial decrease in atherosclerosis when the ABCA1 gene (an LXR α target) was overexpressed [2]. Furthermore, results from this study indicated a reduction in atherosclerosis proliferation, leading to the conclusion that LXR's possess antiatherogenic properties in mice [2]. Therefore, it is possible that synthetic agonists for LXR α could yield beneficial effects for humans as well, potentially reducing circulating triglycerides. However, LXR drugs in particular have been known to cause detrimental side effects in mice and hamsters, such as elevated triglycerides and phospholipids, presumably via the SREBP-1 pathway [10]. Interestingly, deletion of LXR α in mice has effectively eliminated the negative side effect of increased triglycerides, while the beneficial effect of elevated plasma HDL was unaltered [11]. With regards to drug development, this data would suggest that pharmaceutical strategies which lower hepatic LXR's or circumvent the liver, would be a viable approach to treating cholesterol anomalies such as cardiovascular disease [11].

RXR

The retinoid X receptor (RXR) is linked to heterodimer formation with other nuclear receptor proteins. Similar to the other nuclear receptors, RXR has three isoforms: alpha, beta and gamma. Isoform function is not well understood due to the vast network of intrinsic pathways linked to retinoic acid. Studies regarding these three isoforms suggest the alpha isoform is ubiquitously expressed, while the beta and

gamma isoforms are more restricted [12]. Analysis of *in vivo* beta transcripts in early stages of embryonic development and adult tissues suggests that this isoform plays a role in epithelial differentiation [12]. The gamma isoform of this receptor displays increased complexity since expression fluctuates throughout regions of the mesenchyme during embryonic development [12]. The alpha isoform is the focus of this project due to its ubiquitous distribution, suggesting a role in homeostatic pathways linked to LXR α and PPAR α .

With regards to natural ligands, RXR α is known to bind 9-*cis* retinoic acid and can also form homodimers and tetramers in the absence of a DNA template [13]. Furthermore, RXR α is known to form heterodimers with PPAR α and LXR α , both with flexible functionality due to tissue specificity. Interestingly, RXR is sometimes referred to as a “silent” partner since dimerization is not dependent on binding 9-*cis* retinoic acid [14]. However, this effect is not exclusive since RXR can be an “active” partner as well, such is the case for the PPAR-RXR heterodimer, where both proteins exhibit synergistic effects in the presence of ligands [14]. Ligand binding is a point of interest as cellular effects are characteristically mediated through allosteric changes via the ligand-binding domain [14].

The retinoid X receptor uses a specific response element (RXRE) consisting of a direct repeat (PuG(G/T)TCA) [12]. The spacing between this polymorphic motif is variable, ranging from a DR1 to DR5. Heterodimers can form in the presence or absence of DNA where target genes for the RXR α -LXR α and RXR α -PPAR α heterodimers include cholesterol 7 α -hydroxylase (CYP7A1) and apolipoprotein A1 (APOA1), respectively [15]. Target genes specifically for RXR α remain elusive due

to the ubiquitous role of RXR α in metabolic pathways, therefore, regulation of gene expression is a point of interest for synthetic ligand development.

Heterodimers

Each receptor protein can dimerize in three different fashions: PPAR α -RXR α , LXR α -RXR α and PPAR α -LXR α , where natural ligands can influence cholesterol and lipoprotein metabolism. [3]. The present day goal is to manipulate each heterodimer with a synthetic ligand, providing benefits for patients with clinical diseases. In order to determine an effective synthetic ligand for the heterodimer of interest, knowledge of metabolic effects for each heterodimer is imperative.

The PPAR α -RXR α heterodimer is known to target genes pertaining to fatty acid oxidation. This heterodimer is a key component in mitochondrial and peroxisomal β -oxidation where natural ligands include fatty acids and fatty acyl-CoAs, further aiding in pathways regarding high-density lipoproteins (HDL) and low-density lipoproteins (LDL). With respect to synthetic ligands, drugs such as statins function as HMG-CoA reductase inhibitors. By inhibiting HMG-CoA reductase, cholesterol levels are significantly reduced, presumably providing beneficial effects for patients with hypercholesterolemia and hyperlipidemia. Other antiatherogenic compounds have been studied, however, none have been FDA approved due to negative side effects. Current medical treatment for metabolic diseases such as diabetes and atherosclerosis include synthetic ligands such as fibrates, known targets of the PPAR α -RXR α heterodimer, which induce peroxisomal proliferation. Clinical effects of fibrates include a reduction in triglyceride levels and an increase in HDL

levels [1]. Knowledge of these heterodimeric proteins becomes critically important when treating diseases related to cholesterol and lipid metabolism.

Correspondingly, the LXR α -RXR α heterodimer is known to regulate genes pertaining to cholesterol metabolism. This heterodimer is tissue specific, meaning biological effects can differ depending on tissue type. For example, in the intestine, LXR α -RXR α may assist in cholesterol reabsorption and excretion whereas in the liver, it may aid in bile acid synthesis [6]. Overall, cholesterol levels throughout the body can be regulated via the LXR α -RXR α heterodimer. These natural processes are affected by endogenous ligands including oxysterols and hydroxycholesterols, where ligand binding initiates transcription. With regards to medicinal research, synthetic counterparts include antiatherogenic compounds such as ticlopidine, nicotinic acid etofibrate, which are designed to achieve metabolic effects similar to natural processes. Currently, there are no drugs on the market known to target this particular heterodimer due to highly adverse side effects.

It has been shown that nuclear receptor proteins PPAR α and LXR α dimerize as well [3], for which cellular effects are not fully understood. Recent data suggests this heterodimer regulates genes targeting cholesterol lipoprotein metabolism. Furthermore, it has been shown that LXR α ligands improve effects caused by the PPAR α -LXR α heterodimer, directly impacting the formation of other heterodimers as well [3]. Accordingly, it has been discovered that the formation of PPAR α -RXR α and LXR α -RXR α are greatly reduced with the addition of PPAR α and LXR α agonists, respectively [3]. This knowledge becomes acutely important when treating patients with synthetic ligands targeting cholesterol or fatty acid pathways pertaining

to diabetes. Since effects of the PPAR α -LXR α heterodimer are relatively unknown, it is possible that current drugs directly affect this heterodimer and have effects on unanticipated cellular processes that are potentially detrimental to the cell. Therefore, knowledge of synthetic ligands and their corresponding *in vivo* effects is a key interest for novel drug discovery.

Cross Talk

Nuclear receptor proteins, PPAR α , LXR α and RXR α , are intrinsically linked where one protein can affect the dimerization and transcriptional activities of another heterodimer pair. Previous discoveries indicate PPAR α can negatively affect the formation of the LXR-RXR heterodimer, down-regulating the SREBP-1c genetic pathway targeted by LXR [16]. The human body displays an abundance of coordinated metabolic networks, specifically regarding fatty acid synthesis and storage. Utilization and storage of fatty acids is a reciprocally coordinated process, regulated by cross-talk between nuclear receptors, further complicating synthetic ligand discovery [16]. Interestingly, the addition of a LXR ligand causes an increase in LXR α -PPAR α heterodimer formation, while the addition of both PPAR α and LXR agonists result in simultaneous reduction of heterodimer formation regarding PPAR α -RXR α and LXR α -RXR α [3]. Cross-talk between these receptors allows for a coordinated control of regulatory genes providing metabolic homeostasis throughout the body. This cross-talk also adds another level of complexity to human cholesterol and fatty acid metabolism, complicating pharmaceutical development for diseases

such as atherosclerosis and diabetes. Accordingly, therapeutic treatment requires extensive scrutiny since drug targets may not be exclusive.

Ligand-Binding Domain

Ligand binding is crucial for initiation of cellular effects via transcription. Binding sites are often specific to a certain ligand in terms of secondary structure or spatial geometry, and are a point of interest for drug development. With regards to ligand binding, nuclear receptor proteins contain ligand-binding sites consisting of alpha helices [2]. Nuclear receptors also contain DNA binding sites composed of zinc finger motifs [2]. Interestingly, the presence of DNA is not required for dimerization, however, DNA binding is enhanced when both domains are present. Ligand binding for these proteins is driven by the C-terminal ligand-binding domain (LBD), acting as a guide for the recruitment of co-activator complexes, leading to gene regulatory functions such as histone methyltransferase and nucleosome remodeling [2]. Correspondingly, without the presence of a ligand, nuclear receptor heterodimers are known to inhibit transcription via co-repressors [2]. The significance of ligand-binding transcriptional effects is an attractive topic for further study, especially with regards to synthetic ligands, leading to potential cures for metabolic diseases linked to obesity and diabetes.

Synthetic ligands are often designed as an agonist or antagonist, targeted for either activation (agonist) or inhibition (antagonist) of certain genes. If an agonist or antagonist can be made to look similar to a natural ligand, it is possible that the ligand can bind to a nuclear receptor and affect transcription. As these ligands bind, the

nuclear receptor proteins undergo a conformational change, altering protein function via transcriptional effects. In the case of an antagonist, conformational changes may occur where the natural ligand can no longer fit into the binding pocket. This could benefit diseases, such as atherosclerosis, where negative metabolic effects may be inhibited. Alternatively, an agonist could work to activate pathways, which may not normally be active, leading to beneficial effects for diseased patients. Pharmaceutical development is influenced by knowledge of ligand binding, leading to discoveries pertaining to cholesterol and lipoprotein metabolism.

Natural and Synthetic Ligands

The ligand-binding domain (LBD) of nuclear receptors, PPAR α , LXR α and RXR α , can mediate cellular processes via transactivation and transrepression functions [2]. Interestingly, the ligand-binding domain encodes several functions including dimerization, ligand binding, transactivation and binding to co-repressors and co-activators, thus the LBD plays a significant role in metabolism [17]. Regarding human metabolism, natural ligands such as cholesterol metabolites and fatty acids bind PPAR α and LXR α with lower affinities (micromolar range) than their steroid counterparts (nanomolar range) [2].

Previous *in vitro* studies have utilized surface plasmon resonance (SPR) to study the effects of ligands on heterodimer pairs, specifically regarding the ligand-binding domain [17]. This particular study is one of the only studies that have evaluated the effects of ligands on heterodimer pairs, as opposed to the individual nuclear receptor proteins themselves [17]. Their published data utilized a fibrinate

drug, Bezafibrate, which was shown to have an incremental effect on the LBD of both PPAR α and LXRs [17]. With regards to chemical interactions, it was found that hydrogen bonding was affected while hydrophobic interactions showed no change upon ligand binding [17]. This study was one of the first to show that ligand binding can have an effect upon dimerization, leading to altered genetic expression in a variety of tissues [17].

The three nuclear receptors, LXR α , PPAR α and RXR α , possess several similarities in regards to ligand binding. It is known that the PPAR α -RXR α complex binds to polyunsaturated fatty acids, while the PPAR α -LXR α complex binds to fatty acyl-CoA's. Consequently, it is possible that a ligand for one nuclear receptor protein could also serve as a ligand for a partner nuclear receptor protein. This could have a significant effect on genetic transcription in response to dimerization. Cross-ligand binding suggests that binding may not be exclusive, therefore, it is clinically significant to test specificity of ligand affinity.

Previous lab data identified that ligand binding does affect dimerization, suggesting that ligand binding determines heterodimer choice. It is important to recognize which sets of genes are being affected by certain ligands in order to accurately treat diseases. For example, it is well known that fibrates have an effect on lipoprotein levels by increasing HDL's and decreasing triglycerides, providing beneficial outcomes for patients with hypertriglyceridemia [2]. Since fibrates are known PPAR α agonists, it is largely assumed that the PPAR α -RXR α heterodimer is the main target since genes involving fatty acid oxidation are affected. Yet, it is

possible there could be unexpected effects on genetic targets regulated by the LXR α -PPAR α heterodimer, potentially affecting genes that are not well understood.

The goal of this thesis project is to test multiple synthetic ligands with each of the three heterodimers to evaluate protein-protein binding affinities and other cellular interactions. Knowledge of how these ligands interact with heterodimers formed from PPAR α , LXR α , and RXR α could provide valuable insight for therapeutic medicine. Ligands to be tested include: Auraptene, Ciprofibrate, Fluorobexarotene, GW-6471, Lovastatin, Pravastatin Sodium Salt, UVI 3003 and T-0901317 (Figure 1).

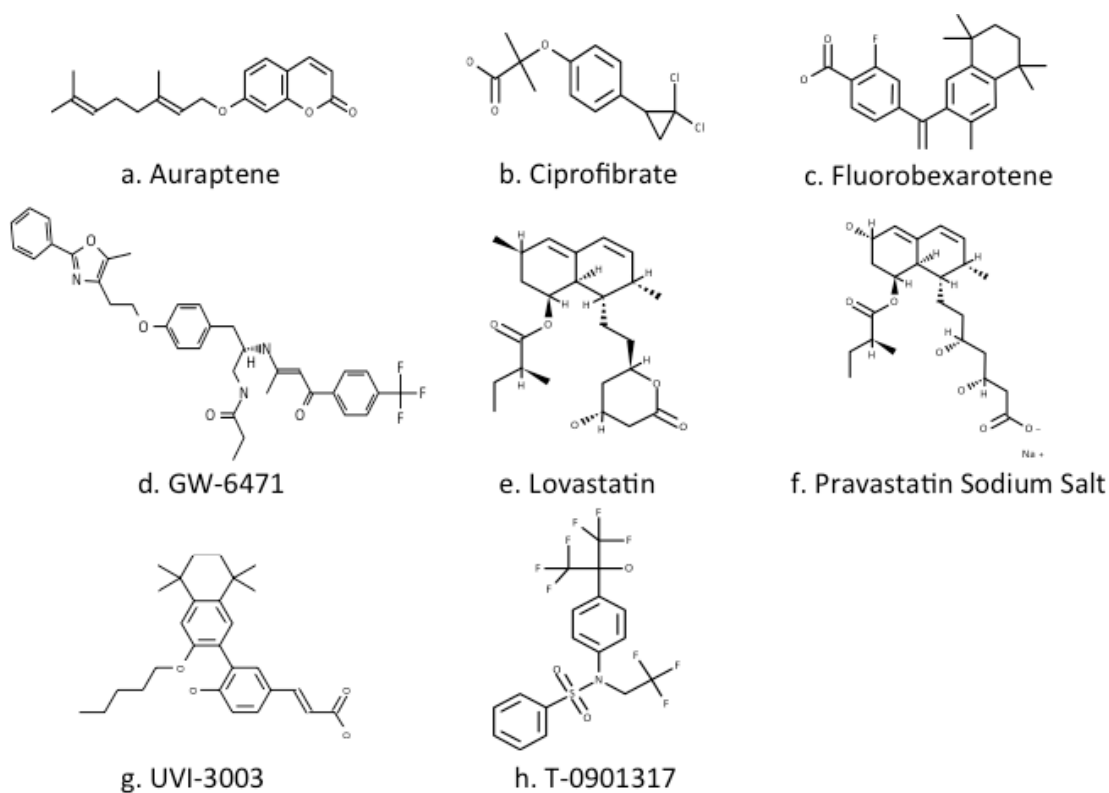


Figure 1. Synthetic compounds and their corresponding structures.

Due to the regulatory role of PPAR α in cholesterol and free fatty acid homeostasis, fibrate drugs have shown the most promise for therapeutic benefit. Currently on the pharmaceutical market, fibrates and statins allow synthetic regulation of free fatty acids and triglycerides, relevant to diabetes and atherosclerosis. Ciprofibrate is one member of the fibrate family, which is a known PPAR α agonist. Previous research has indicated that fibrates can regulate free fatty acids, triacylglyceride homeostasis and lipoprotein levels, making fibrates highly beneficial to hypertriglyceridemic individuals [2]. Fibrates are also known to protect against atherosclerosis by stimulating high-density lipoproteins (HDL) and regulating lipid homeostasis [7]. Fibrates particularly act through the ABCA1 gene, which is responsible for maintaining lipid and cholesterol homeostasis [18]. Accordingly, the

ability of fibrates to target this gene allows for increased transcription, resulting in elevated HDL levels, benefiting patients suffering from atherosclerosis and coronary heart disease [18]. However, fibrate drugs can also cause negative side effects, the most common being gastrointestinal problems [19]. In addition to dyspepsia, fibrates can make patients prone to gallstones due to elevated biliary cholesterol [19]. Furthermore, statins can also have beneficial outcomes for individuals with high cholesterol, inhibiting cholesterol synthesis and promoting the conversion of cholesterol to bile acids. This research will primarily focus on lovastatin and pravastatin sodium salt. Interestingly, previous studies have shown that lovastatin can induce transcription of the gene *CYP7A1*, which codes for an enzyme that participates in the rate-limiting step of bile acid synthesis. Stimulation of this gene allows for elevated bile acid synthesis in the liver, leading to a possible interaction with $LXR\alpha$ [20]. Furthermore, lovastatin and pravastatin sodium salt function as HMG-CoA reductase inhibitors, helping lower cholesterol levels throughout the body. Although these drugs have therapeutic relevance and seemingly beneficial outcomes, the undesired side effects cannot be ignored. It has been shown that statins can induce myopathy, where detrimental effects are worsened when combined with a fibrate [19]. By further understanding the interaction of nuclear receptor proteins with these drugs, side effects could potentially be eliminated, making fibrates and statins invaluable to diabetic patients, as well as patients with fatty acid and cholesterol disorders. Furthermore, these are intriguing drugs to study due to the wide effects on energy metabolism, specifically concerning cross-talk and regulation of the heterodimers formed by $PPAR\alpha$, $LXR\alpha$ and $RXR\alpha$.

Correspondingly, the only antagonist known for PPAR α is GW-6471 (Xu et al), for which very little is known. This drug was originally designed to test the binding of corepressors with PPAR α [21]. Modified from the PPAR α agonist GW-409544, the GW-6471 ligand contains an amide group instead of a carboxylate group, making this a functional PPAR α antagonist [21]. This antagonist functions by disrupting coactivator complexes of nuclear repressors, thus promoting the recruitment of corepressors such as Silencing Mediator for Retinoid and Thyroid hormone receptors (SMRT) and Nuclear CoRepressor (N-CoR) [21]. The hope is synthetic compounds like this could provide symptomatic relief for hypertriglycemic and diabetic individuals with minimal side effects.

Commonly studied RXR agonists include bexarotene, also known as 4-[1-(3,5,5,8,-Pentamethyl-5,6,7,8-tetrahydro-2-naphthyl)ethynyl]benzoic Acid), generically known as Targretin. This drug is currently used to treat patients with cutaneous T-cell lymphoma since it can inhibit metastasis and initiate apoptosis [22]. Current side effects include increased lipid levels and high cholesterol, making this an attractive target for clinical research [22]. Genes involved in lipid homeostasis can be targeted by this compound, including sterol regulatory element-binding transcription factor 1 (SREBP-1c), Stearoyl-CoA desaturase-1 (SCD1), fatty acid synthase (FASN), as well as ATP-binding cassette, sub-family G (ABCG5 and ABCG8) [23]. In fact, the tissue specificity of the LXR-RXR heterodimer was discovered through a study using bexarotene, to observe effects on target genes such as ABCG5 and ABCG8 [23]. By analysis of mRNA levels, it was discovered that expression of these genes differed in the liver and intestine, suggesting tissue specificity of the LXR-

RXR heterodimer [23]. A previous study designed and tested multiple analogues of bexarotene where it was determined that non-hydrogen functional groups, substituted on the aromatic ring close to the carboxylic acid, exhibited increased binding affinity for RXR α [24]. The derivative fluorobexarotene was chosen for study due to a 75% increase in binding affinity when compared to bexarotene alone, which was the greatest of all analogues tested [24]. It was determined that this novel RXR α ligand also demonstrates minimal activity as an RAR agonist, thus negative side effects may be lessened in therapeutic use. Target genes affected by fluorobexarotene are unknown, however, it is likely that genetic regulation is similar to that of bexarotene since the molecular structures are similar.

Correspondingly, an RXR antagonist was chosen for study as well. The particular RXR antagonist chosen, UVI-3003, has been previously used to study the specific role of RXR in the differentiation of adult alveolar epithelial cells, for which research is still in its infancy [25]. The goal of this previous study was to determine if RXR was acutely responsible for epithelial cell differentiation in human lungs by inhibiting RXR effects using UVI-3003 [25]. It was determined that RXR is responsible for cellular differentiation, however, unequivocal results can be difficult to obtain since RXR plays a role in biological processes such as the transforming growth factor beta (TGFB) and hepatocyte nuclear factor 4 alpha (HNF4A) pathways [25]. Even though little is known about the specific function of RXR, it has been shown that cells can be rescued from antagonizing effects seen with UVI-3003, suggesting that potential negative side effects of this medication could be reversed [25]. Yet, the precise point of regulation is highly dependent upon protein-protein

interactions within the cell, therefore, it is necessary to study the effects of these drugs on heterodimers formed by PPAR α , LXR α and RXR α to better understand regulatory effects, relevant to therapeutic medicine.

Regarding LXR α , a well-studied synthetic ligand of interest is the T-0901317 compound [26]. Previously discovered target genes include: ABCA1, acetyl-CoA carboxylase, SCD1, SREBP-1c and FAS [26]. The T-0901317 ligand functions as an agonist for LXR α , providing treatment for clinical patients suffering from low levels of HDL's [26]. Although this ligand has therapeutic relevance and seemingly beneficial outcomes such as elevated HDL levels, the undesired side effects cannot be ignored. None of the drugs targeting LXR α have been FDA approved due to negative side effects. For example, the T-0901317 compound can induce lipogenesis leading to an increase in HDL's, resulting in elevated liver and plasma triacylglycerols [26]. Studies have shown that these negative effects in plasma are transient, however, detrimental effects of triacylglycerol levels in the liver are less understood [26]. Furthermore, this LXR α agonist has been shown to decrease atherosclerosis in mice by lowering hepatic cholesterol [11]. While some studies hold promise for success, it is still important to understand which cellular processes are being targeted in regards to transcriptional regulation via heterodimers formed by RXR α , LXR α and PPAR α . This is especially necessary in therapeutic medicine to achieve a high success rate, with minimal adverse side effects.

Ligands of clinical significance are not exclusively synthetic; one unique biochemical compound of interest has been proposed to target LXR α , exhibiting antagonizing effects [27]. This compound, auraptene, is classified as a citrus

phytochemical and exists as a monoterpene coumarin ether [27]. Auraptene, isolated from *Citrus ichangensis* peel extract, has been shown to arrest triglyceride and lipid proliferation in adipocytes, thus providing benefits for patients suffering from metabolic disorders related to obesity [27]. Interestingly, auraptene appears to have more than one nuclear receptor target. Derivatives of this compound can affect LXR target genes by inhibiting expression of genes such as apolipoprotein E (ApoE), cytochrome P450 7A1 (CYP7A1), and lipoprotein lipase (LPL), suggesting auraptene functions as an LXR antagonist [27]. With regards to PPAR, the ability of auraptene to restore insulin sensitivity and regulate glucose homeostasis demonstrates complex regulation of PPAR α and PPAR γ , suggesting auraptene could act as a general PPAR agonist [27]. Furthermore, auraptene derivatives were shown to decrease expression of PPAR γ target genes such as fatty acid synthase (FAS), acyl-CoA oxidase (ACOX) and uncoupling protein 2 (UCP2) [27]. Since auraptene derivatives exhibit cross-talk between PPAR and LXR, it is possible that auraptene binding is not exclusive and multiple receptors could be affected. This promiscuous binding could result in unforeseen negative side effects, leading to complications in therapeutic treatment of diseases related to obesity and diabetes.

Ligand-binding is a point of interest and can affect multiple aspects of heterodimer formation such as stereochemistry, binding affinity and protein-protein interactions. Accordingly, evaluation of the novel heterodimer PPAR α -LXR α can provide valuable insight into therapeutic treatment regarding obesity and diabetes, allowing for a deeper understanding of pharmaceutical repercussions and side effects.

II. HYPOTHESIS AND AIMS

Experimental techniques will be utilized to evaluate the **hypothesis that ligand binding determines the relative binding affinities and subcellular localization of nuclear receptors**. Procedures and techniques used to test this hypothesis will focus on the heterodimer pair formed by PPAR α and its partner receptor LXR α .

Aim 1: The goal is to determine if synthetic ligands modulate the formation of heterodimer pairs.

Protein-ligand interactions will be evaluated using intrinsic fluorescence quenching to establish ligand exclusivity. Additionally, fluorescence resonance energy transfer (FRET) will be primarily used to evaluate effects of synthetic ligands on protein-protein interactions. These assays will help narrow the scope of drugs to be tested in aim 2. Ligands that induce significant changes in the binding affinities of heterodimeric partners will be utilized for further testing. Circular dichroism will be implemented to test for differences in secondary structures caused by ligand binding and protein dimerization.

Aim 2: The goal is to determine the effects of ligands on subcellular localization of PPAR α , LXR α and RXR α .

Bimolecular fluorescence complementation (BiFC) will be used to visualize the effects of ligands on subcellular localization *in vivo* using COS-7 cells. Cells transfected with BiFC fusions of PPAR α and LXR α will be used to evaluate the hypothesis. Fluorescence microscopy provides an *in vivo* assay where subcellular localization of heterodimer pairs can be visualized based on quantitation of fluorescence.

III. MATERIALS AND METHODS

Plasmid Construction for hPPAR α , hLXR α and hRXR α

All experiments employed the use of full-length human PPAR α , LXR α and RXR α . Expression plasmids were pre-existing in the lab, and were constructed using the methods described below. Plasmids for producing purified proteins were constructed by adding an N-terminal polyhistidine tag (six His residues) to the Glutathione S transferase (GST) open reading frame in the pGEX6P vector (Amersham Biosciences, Piscataway, NJ) via overlap polymerase chain reaction (PCR). The result consists of six histidine residues and a GST tag upstream of a PreScission Protease site and a multiple cloning site, amplified from complimentary DNA [28, 29]. Each nuclear receptor was derived from HepG2 cells using appropriate primers as shown in Figure 2.

- A 5'-cggatccATGGTGGACACGGAAAGCCC-3'
 5'-cgtcgacCTATCAGTACATGTCCCTGTAG-3'
- B 5'- ggatccATGTCCTTGTGGCTGGGGGCCCCTGTG-3'
 5'-aagcttCTCGAGTCATTTCGTGCACATCCCAGATCTC-3'
- C 5'-cgaattcATGGACACCAAACATTTCTGCCGCT-3'
 5'-ctcgagCTAAGTCATTGGGTGCGGCGCCTCC-3'

Figure 2. Primers used for amplification from cDNA derived from HepG2 cells. (A) Primers used for hPPAR α . **(B)** Primers used for hLXR α . **(C)** Primers used for hRXR α . Nucleotides outside of the target sequence are represented by lower case letters with the restriction site underlined.

Following PCR, the products were cloned into the pGEM-T easy vector (Promega Corporation, Madison, WI) for sequencing and subsequently transferred into the *Bam HI/Sall*, *BamHI-HindIII* or *EcoRI-XhoI* sites of the pGEX-6P derivative to produce 6xHis-GST-hPPAR α (Figure 3A), 6xHis-GST-hLXR α (Figure 3B) and 6xHis-GST-hRXR α (Figure 3C), respectively [28, 29]. These ampicillin-resistant plasmids were further transformed into Rosetta 2 competent cells for protein expression.

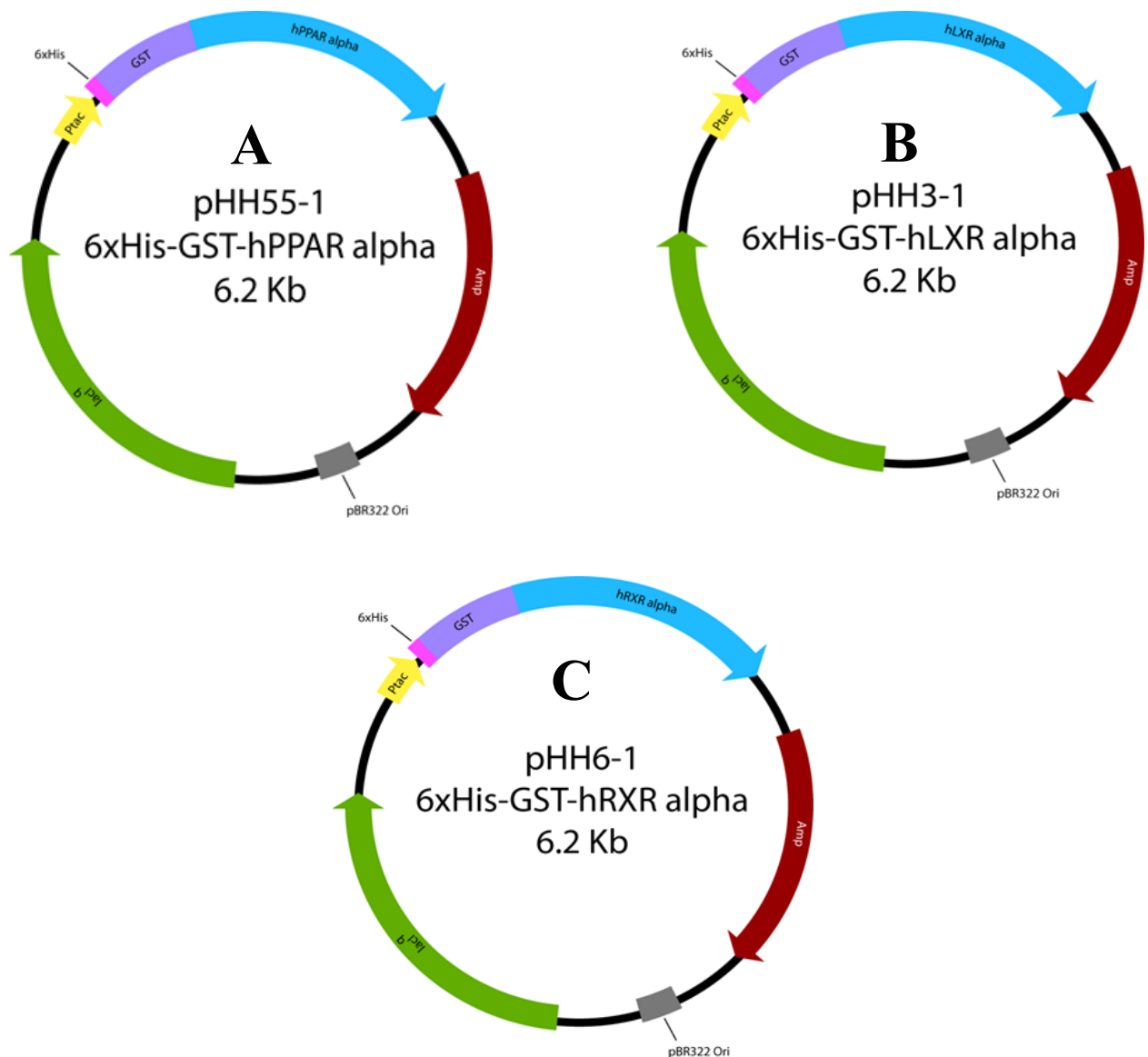


Figure 3. Schematic of plasmid DNA constructs for full-length His-tagged proteins. (A) Representation of the cDNA encoding hLXR α , constructed by adding an N-terminal polyhistidine tag (six His residues) to the Glutathione S transferase (GST) open reading frame in the pGEX6P vector. (B) Representation of the cDNA encoding hPPAR α , constructed by adding an N-terminal polyhistidine tag (six His residues) to the Glutathione S transferase (GST) open reading frame in the pGEX6P vector. (C) Representation of the cDNA encoding hRXR α , constructed by adding an N-terminal polyhistidine tag (six His residues) to the Glutathione S transferase (GST) open reading frame in the pGEX6P vector.

Recombinant Protein Purification

i. Protein Expression in Escherichia coli

Plasmids for recombinant protein expression were transformed into Rosetta 2 competent cells (Novagen), plated onto selective media and incubated at 37°C overnight. For each protein, an overnight bacterial culture of 200 ml was grown from 5 colonies at 30°C and shaken at 200 rpm in Luria Bertani (LB) media (Sigma Aldrich) containing 10% glucose, 2 mg chloramphenicol and 10 mg ampicillin. The following morning, the 200 ml culture was sub-cultured into two 1L flasks containing LB (100 ml culture per 1L) and propagated at 37°C for approximately 3 hours or until the optical density (OD600) reached 1.1-1.3. After achieving the proper OD, 1 ml of 0.1M isopropyl β -D-1-thiogalactopyranoside (IPTG) was used in each liter to induce protein expression where the resulting mixture was allowed to incubate at 16°C for 4 hours. Subsequently, bacterial cells were pelleted by centrifugation, using an Avanti-J26 XPI centrifuge JA-10 rotor, at 4°C with a speed of 8500 rpm for 10 minutes. Following centrifugation, 100mM of protease inhibitor, phenylmethylsulfonyl fluoride (PMSF), was added to each pellet and stored at -80°C overnight.

ii. Purification via Affinity Chromatography

Protein purification was conducted by applying a soluble protein fraction to a glutathione cartridge (Bio-Rad Inc.); followed by washes and on-column cleavage of the GST tag. A soluble protein fraction was created by re-suspending the pellet from a 1L culture in 10 ml of 2X L&C buffer (2500mM Tris, pH 8.0, 20% glycerol and 590mM NaCl), 500mM EDTA, 100mM DTT and 10 ml 2X protease inhibitor

(SIGMAFAST™ protease inhibitor cocktail tablet, EDTA-free, Sigma-Aldrich). The bacterial cells in the resulting mixture were lysed via sonication at 6 intervals of 30 seconds on/off at 50% amplitude using a Fisher Scientific© sonic dismembrator, model 150E. The mixture was then centrifuged using an Avanti-J26 XPI centrifuge with a JA-25.50 rotor at 10,000 rpm for 30 minutes. The cell lysate was collected and filtered using a 1.2 micron filter, loaded onto the glutathione column and purified by affinity chromatography. A flow rate of 0.1 ml per minute was used for loading the column and for subsequent washes. First, the column was allowed to equilibrate with 5 ml of 1X L&C buffer (25000mM Tris, pH 8.0, 20% glycerol and 590mM NaCl). Secondly, an ATP buffer (5 ml consisting of 2X L&C buffer, 10mM ATP and 50mM MgCl₂) was applied, followed by a third buffer consisting of 10 ml 1X L&C (containing 0.5mM EDTA and 1mM DTT), thus removing any unbound protein from the column. In order to elute the bound protein of interest from the GST column, a mixture of PreScission protease (1 ml 1X L&C, 0.5mM EDTA, 120 ug protease, 1mM DTT) was applied. Elutes were collected in 1 ml fractions containing 10% glycerol and 200 µl of 5M NaCl to promote protein stability. To ensure complete removal of pure protein from the GST column, multiple 1 ml elutes were collected.

iii. Protein Concentration and Purity

After collecting elutes, protein concentrations were determined via a Bradford assay (Bio-Rad Inc.) where 5 µl of sample was mixed with 195 µl of Bradford reagent (Bio-Rad Inc.). Resulting values were compared against bovine serum albumin (BSA) standards (Sigma Aldrich) ranging from 0.1 mg/ml to 0.8 mg/ml, where a

spectrophotometer was used to record absorbance measurements at 595 nm. Accordingly, tabulation of results allowed for extrapolation of absorbance values which were compared against a set of standards to yield a linear equation of the form $y = mx + b$. Using this equation, protein concentrations of eluted fractions were established. These protein fractions were further concentrated by centrifugation using a 30KDa or 10KDa filter. The degree of concentration was dependent on experimental parameters for optimal effectiveness.

Protein purity was established by sodium dodecyl sulfate polyacrylamide gel electrophoresis (SDS-PAGE) with Coomassie blue staining. Protein samples from each stage of the purification process were treated with 2X sample buffer containing 100mM DTT and heated at 90°C for 3 minutes. Samples were promptly loaded onto a 10-12% polyacrylamide gel along with a pre-stained benchmark protein ladder (Invitrogen). The gel was run at a constant amperage of 30V for 60 minutes in 1X electrode buffer containing 10% SDS and then imaged using a Fujifilm LAS-4000 CGR (imaging system) in the Wright State University center for genomics research.

Protein-Protein Interactions *in vitro*

i. Ligand-Binding Assays

The first step in this process is to study ligand-binding behavior with a single protein by measuring binding affinities using a photon counting spectrofluorimeter (PC1). It is essential to test binding affinities for each ligand with each nuclear receptor alone to determine if binding really is exclusive. For example, it is possible that a PPAR α agonist, such as ciprofibrate, could potentially bind to LXR α , drastically affecting gene targets. Upon further evaluation of heterodimer pairs and protein-protein interactions, knowledge of ligand exclusivity becomes critically important. This phenomenon may provide an explanation for negative side effects of pharmaceutical compounds, leading to a better understanding of therapeutic treatment for diseases linked to obesity and diabetes.

A photon counting spectrofluorimeter (PC1) was used to measure protein-ligand interactions *in vitro*, establishing binding affinities for each ligand tested. The PC1 can measure intrinsic protein fluorescence by exciting tyrosine and tryptophan residues at 280nm, where resulting peak emission values can be used to plot the change in fluorescence upon titration with a ligand. A saturable curve is indicative of binding, and can be used to estimate the dissociation constant (K_d). Alternatively, a straight line suggests either non-specific binding or lack of binding for a particular ligand. Furthermore, a double reciprocal plot can be utilized to determine the number of binding sites on a particular protein. A linear double-reciprocal plot demonstrates a single binding site, whereas a sigmoidal curve suggests two or more binding sites. This information is beneficial in determining the affinity of a particular ligand for a

certain protein, providing valuable insight to further understand effects of molecular homeostatic pathways. Samples were excited at 280nm with a bandwidth of 0.8mm. Emission wavelength was scanned over a range of 310-370nm also using a bandwidth of 0.8mm. All scans were completed without a polarizer using 1mm slits at a constant temperature of 24°C. The protein of interest was titrated with increasing amounts of ligand, while readings were taken in intervals of 3 minutes. For each binding experiment, the concentration of protein was verified using a Bradford protein assay (Bio-Rad Inc.) to ensure accurate measurements. Each experiment utilized protein fractions at a concentration of 100nM, while sequential ligands were prepared at a concentration of 100µM in DMSO and titrated up to 300nM in increasing increments. Molar increments were optimized such that more readings were taken in the lower nanomolar range (0-50nM) where binding was most likely to occur.

ii. Circular Dichroism (CD)

Circular dichroism is a technique that allows for characteristic, structural analysis of a given protein. The far UV region (240-180nm) provides information on secondary structure (α helices, β sheets, turns and unordered structures), since the peptide bond is the principal absorbing group [30]. Alternatively, the near UV region (320-260nm) presents data regarding tertiary structure due to absorption of aromatic amino acid side chains [30]. With regards to clinical application, this technique has enabled discoveries in degenerative diseases such as bovine spongiform encephalopathy (BSE), scrapie and Alzheimer's disease since the formation of β -

sheets serves as a precursor to the formation of amyloid fibrils, which are characteristic markers of these diseases [30]. Furthermore, this technique can be used to identify changes in protein structure upon the addition of certain drugs or ligands.

Circular dichroism was used to study structural changes in the hLXR α -hPPAR α heterodimer in response to synthetic ligands using a J-815 spectropolarimeter (JASCO Inc.). Previously, secondary structures of individual proteins were analyzed with endogenous ligands, using the human glucocorticoid receptor (hGR) as a negative control [29]. While previous studies focused on analyzing individual nuclear receptors, this experiment focused on synthetic ligand effects regarding the novel heterodimer, hLXR α -hPPAR α . Synthetic ligands used in this study were: fluorobexarotene, ciprofibrate, T-0901317, auraptene and GW-6471. All compounds were dissolved in 50% DMSO, except for T-0901317 which was dissolved in ethanol. Each compound was prepared at a concentration of 100 μ M.

Ionic strength must be considered when using circular dichroism because the ionic strength of a solution in a reaction cuvette can create voltage spikes if the salt concentration is too high. Proteins were concentrated to minimize the volume of sample added to the reaction cuvette, therefore decreasing the total ionic strength of the system. Buffer solutions are an important consideration for circular dichroism since many salt molecules, such as chloride ions, affect pH and absorb strongly below 195 nm [30]. Therefore, to minimize absorbance by excessive salt, proteins were concentrated to 0.40 mg/ml (hLXR α) and 0.53 mg/ml (hPPAR α) in PBS buffer. For all samples, the amino acid concentration was kept at 0.0003M to achieve an absorbance intensity of 0.8 within the range of λ = 180-260 nm. Circular dichroic

spectra were obtained for individual proteins hPPAR α (0.60 μ M) and hLXR α (0.60 μ M), alone and in the presence of synthetic ligand (5 μ M). More importantly, effects of synthetic ligands on secondary structure of the novel heterodimer, hLXR α -hPPAR α , were analyzed by using 0.3 μ M hPPAR α and 0.3 μ M hLXR α , alone and in the presence of ligand (5 μ M). Data for each replicate was collected using a continuous scan over the far-UV range (180-260 nm) with a bandwidth of 1.0 nm at a scan rate of 50 nm/min. Five scans were averaged for each sample and secondary structure composition was compared against a CD Pro, software database using the programs CONTIN and SDP42. Estimates for α -helices, β -sheets, turns and unordered structures were established and statistically analyzed using a two-way t-test in Sigma Plot $\text{\textcircled{C}}$. Furthermore, molar ellipticity was plotted as a function of wavelength to yield characteristic spectra for each sample set. Heterodimeric structure was compared both with and without the presence of ligand to determine unique effects of synthetic ligands on the hLXR α -hPPAR α heterodimer.

Each protein alone yields a characteristic CD spectra from which computational analysis can be established from an average of five scans. If two proteins interact, the spectra and the estimated composition would presumably be altered. Such is the case with LXR α and PPAR α during the formation of a heterodimer. Additional changes in secondary structure could be induced by a synthetic ligand, resulting in an altered CD spectrum. If a synthetic ligand were shown to alter the binding affinity of LXR α and PPAR α , a change in the CD spectra and estimated composition of α -helices, β -sheets, turns and unordered structures would be expected.

iii. Fluorescence Resonance Energy Transfer (FRET)

To investigate effects of synthetic ligands on protein-protein interactions between LXR α and PPAR α , fluorescence resonance energy transfer (FRET) studies were completed. Fluorescence resonance energy transfer consists of two fluorescently labeled proteins, which exclusively produce a fluorescent signal upon dimerization when excited at the appropriate wavelength. Each protein bears a fluorescent label and the two labels represent a “FRET pair.” As these proteins dimerize, there is an energy transfer from the donor molecule to the acceptor molecule, for which fluorescence changes can be visualized. In order for energy transfer to be seen as a change in fluorescence, it is important that the spectra for the donor and acceptor molecules overlap slightly, such that a decrease in donor emission can be seen, along with an increase in acceptor emission [31]. As an alternative to intrinsic quenching assays, FRET studies utilize extrinsic fluorophores to view changes in fluorescence, and are suitable for a variety of applications such as intermembrane interactions and the study of viral protein envelopes [31].

In order to complete FRET studies regarding nuclear receptor proteins, LXR α , PPAR α and RXR α , each protein must be fluorescently labeled with an extrinsic dye. Characteristically in the past, cyanine dyes such as Cy3 and Cy5 have been used to study fluorescence quenching via FRET assays [29]. This particular labeling technique caused complications due to environmental instability of the fluorophores, where conformational changes upon protein dimerization, produced fluorescent changes that were greater than effects seen by fluorescence quenching. Therefore, Alexa Fluor dyes were selected for labeling due to greater environmental stability,

high quantum yield and low solvent sensitivity. Chemically, the Alexa Fluor dyes were covalently attached to nuclear receptor proteins on primary amines. Proteins were labeled using Alexa Fluor microscale labeling kits (Invitrogen) in combination with 3ml slide-a-lyzer G2 dialysis cassettes (Fisher Scientific). Prior to labeling, proteins were dialyzed in PBS (pH 7.5) such that the final buffer did not contain any primary amines (ammonium ions, Tris, glycine, ethanolamine, triethylamine or glutathione). Protein concentration prior to labeling was near 1 mg/ml to ensure adequate labeling. To establish proper pH for the labeling reaction, 1/10 volume of a 1M sodium bicarbonate solution was added to the unlabeled protein. Subsequently, the appropriate amount of dye was added to the protein mixture and allowed to incubate at room temperature for 15 minutes. The resulting solution was transferred to a dialysis cassette and allowed to dialyze in 1L of high salt PBS buffer (Table 1). The buffer was changed four times before the protein was removed and aliquotted for FRET experiments. After labeling, the concentration and degree of labeling were determined for each Alexa Fluor dye reaction. Ideally, a dye to protein ratio would be 1:1 for each reaction, meaning one dye molecule would be attached to one protein molecule. Therefore, the degree of labeling value would be close to 1. The degree of labeling was between 1 and 2 for all sequential experiments regarding PPAR α and LXR α .

Table 1. Composition of high salt PBS buffer

Salt	Concentration
Sodium Chloride	150mM
Potassium Chloride	2mM
Sodium Phosphate (dibasic)	10mM
Potassium Phosphate (monobasic)	1.7mM
De-ionized water	To 1L

Prior to adding synthetic ligands, it was necessary to determine which dye-protein combinations would be most suitable for FRET, since some may be more applicable than others. Three Alexa Fluor (AF) dyes were chosen for study: AF-488, AF-555 and AF-594. Preliminary control tests were completed using a fluorescently labeled protein in the absence of ligand, such as Alexa Fluor 488-labeled human LXR α (AF-488hLXR α), titrated with unlabeled protein such as hPPAR α . Similar tests were done for all three fluorescently labeled proteins to determine which dye-protein combination produced a minimal change in fluorescence upon dimerization. This would suggest that changes seen from FRET would be a direct result of future ligand interaction, as opposed to natural conformational changes upon dimerization, caused by the extrinsic fluorophore. The ultimate goal was to use two fluorescently labeled proteins, demonstrating a minimal change in fluorescence upon dimerization, to study the effects of a given synthetic ligand. These studies provided valuable insight to protein-protein interactions in response to pharmaceutical compounds both on and off the market.

Protein-Protein Interactions *in vivo*

Direct visualization of cellular effects *in vivo* can provide valuable insight to protein-protein interactions. This approach can be implemented using bimolecular fluorescence complementation (BiFC); a widely accepted technique resulting in a direct readout and elevated complementation signal [32]. Bimolecular fluorescence complementation utilizes a single fluorophore split into two parts, creating N-terminal and C-terminal fragments [32]. These assays can be used to view intracellular effects in response to an added ligand, either synthetic or natural. For example, a previous study utilized two fragments of the yellow fluorescent protein to study the effects of intracellular calcium on the M13 calmodulin binding peptide, and calmodulin itself [33]. By using fluorescence microscopy, this technique can be utilized to visualize changes in fluorescence intensity and nuclear fluorescence. Without external ligands, fluorescence would likely be seen in the nucleus, however, when synthetic ligands are introduced, fluorescence may migrate to other parts of the cell.

With regards to this project, in the past, the cerulean fluorescent protein (Cfp) was utilized to observe nuclear fluorescence upon protein-protein dimerization. The N-terminal region of the Cfp protein was covalently attached to hPPAR α , which was the central protein for this study. Additionally, the C-terminal regions of the other two proteins (hLXR α and hRXR α) were covalently labeled with a mutated Cfp fluorophore, termed Venus and Cerulean, respectively. Modifications of this fluorophore resulted in a brighter color, where resulting heterodimers produced a yellow signal (hLXR α -hPPAR α) and a blue signal (hPPAR α -hRXR α) (Figure 4). Additional preliminary experiments employed the same concept, except hLXR α was

made the central protein. Resulting nuclear fluorescence produced a yellow color for hLXR α -hPPAR α and a blue color for hLXR α -hRXR α . In order for BiFC to be effective, it is important to know that intrinsic fluorescence is a direct result of protein-protein interaction and not due to the fluorophores themselves [33]. Accordingly, it was determined that visualization of fluorescence was a direct result of protein-protein dimerization. Predominantly, the goal of this technique was to study subcellular localization in the nucleus via fluorescence microscopy, both with and without synthetic ligands. Changes in fluorescence location and intensity were measured, providing useful data to deepen the understanding of these nuclear receptors and their role in therapeutic medicine.

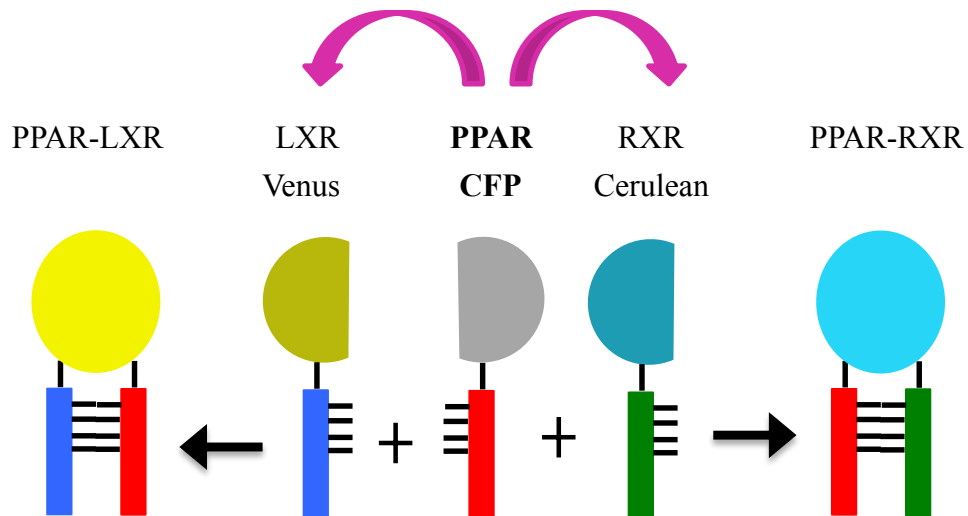


Figure 4. Schematic of BiFC constructs where hPPAR α is the central protein. The N-terminus of the Cfp protein is covalently attached to PPAR α . The C-terminal regions of Venus and Cerulean are covalently attached to LXR α and RXR α , respectively. When PPAR α and RXR α dimerize, a blue color is produced. When LXR α and PPAR α dimerize, a yellow color is produced. Image Adapted from C. D. Hu and T. K. Kerppola, *Nat. Biotechnol.*, 2003, **21**, 539.

i. COS-7 Stable Transfection

Conjointly, COS-7 cells were transfected with three plasmids encoding for Venus-hLXR α (Figure 5A), Cerulean-hRXR α (Figure 5B), and ECFP-hPPAR α (Figure 5C). Stable cells were selected via antibiotic resistance, where the goal was to locate cells which stably integrated all three plasmids. It is possible that some cells only integrated one or two plasmids, resulting in potential skewed experimental results when introducing ligands. Upon the addition of ligands, it is important to know any changes seen in fluorescence microscopy are exclusively due to synthetic ligands themselves and not because plasmid integration was a temporary effect. Stable cells were evaluated using polymerase chain reaction (PCR) to verify the presence of all three plasmids.

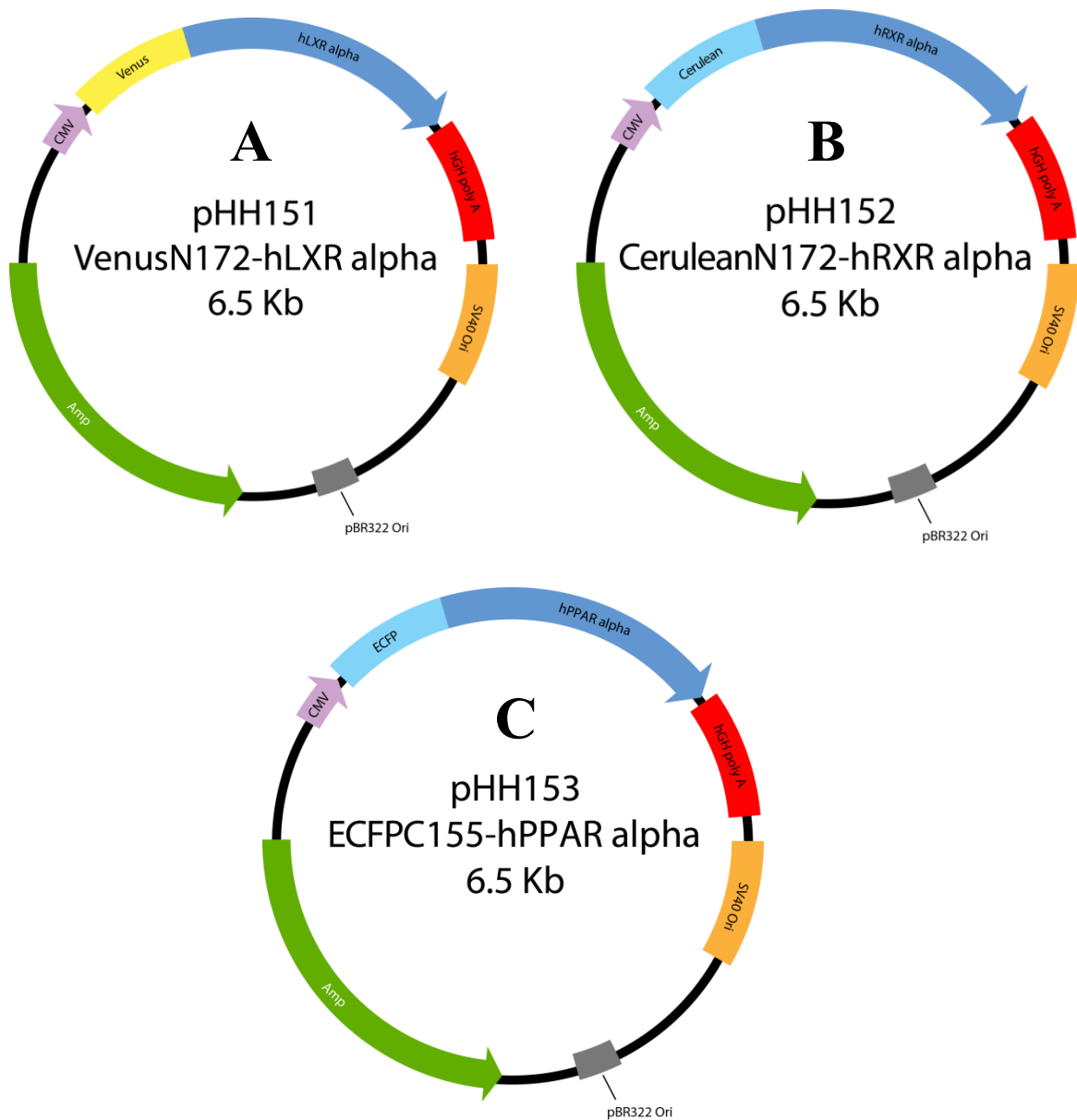


Figure 5. Schematic of plasmid DNA construction for bimolecular fluorescence complementation using stable transfections. (A) Plasmid pHH151 coding for VenusN172-LXR α using the ampicillin resistance gene and a CMV promoter. (B) Plasmid pHH152 coding for CeruleanN172-RXR using the ampicillin resistance gene and a CMV promoter. (C) Plasmid pHH153 coding for ECFPC155-PPAR α using the ampicillin resistance gene and a CMV promoter. Plasmids were transfected into COS-7 cells resulting in stable transfections.

ii. DNA Isolation

Dishes of BiFC COS-7 cell clones were treated with 500 μ l isolation buffer (100mM Tris, 1% SDS and 100mM EDTA) and DNA was isolated via chloroform extraction. To isolate cellular DNA, cell lysates were treated with 1.5 μ l ribonuclease (10 mg/ml), incubated at 42°C for 20 minutes, followed by 12 μ l proteinase K (10 mg/ml), incubated at 65°C for 30 minutes. Subsequently, lysates were treated with 500mM potassium acetate and allowed to chill at -20°C for 10 minutes. Each tube was centrifuged at 14,000 rpm for 5 minutes and the resulting supernatant was collected in a fresh microcentrifuge tube. Exactly 550 μ l of Phenol:chloroform:Iso-amyl (25:24:1) solution was added to the supernatant, mixed and centrifuged at 14,000 rpm for 3 minutes. Again, the supernatant was transferred to a fresh tube and treated with 50 μ l of 300mM sodium acetate, filled to 1 ml with 100% ethanol and was allowed to chill at -20°C for 20 minutes. Then, the ethanol was carefully removed and the DNA pellet was allowed to air dry. Lastly, the dried DNA pellet was re-suspended in 40 μ l of 0.1X TE (10mM tris, 1mM EDTA, pH 8.0).

iii. Polymerase Chain Reaction

Isolated DNA was added to GoTaq Green Master Mix (Promega) and treated with appropriate primers. The primer set used for this study contained a 5' end which bound to the BiFC region of the plasmid and a 3' end which bound to the nuclear receptor. Primers were designed in this fashion to ensure amplification of the nuclear receptor, which was covalently linked to the appropriate BiFC fragment. Accordingly, the DNA was denatured at 94°C while primers were allowed to anneal

at 58°C. Sequentially, primer extension was completed at 72°C and the polymerase chain reaction process was allowed to cycle 35 times before evaluating via electrophoresis. To visualize the amplified DNA of interest, resulting mixtures were run on a 1% Agarose gel in 0.5X TBE buffer at 150V for 45 minutes and imaged on a Fujifilm LAS-4000 CGR (imaging system) in the Wright State University center for genomics research. Results allowed detection of cells, which contained all three plasmids for further *in vivo* studies.

iv. COS-7 Transient Transfections

Transient transfections were implemented due to complications with the stably transfected cells. Analytical details regarding these difficulties are outlined in the results section. In order to create transiently transfected cells, live COS-7 cells were first seeded on LabTek II chambered coverslips from 10-cm, confluent (80-90%) dishes of wild type COS-7 cells. Each chamber received 0.5 ml of cells and 1 ml of fresh media (Dulbecco's Modified Eagle Medium). Cells were transiently transfected with 0.9 µl Venus-hLXRα (Figure 5A), 0.6 µl Cerulean-hRXRα (Figure 5B), and 1.0 µl ECFP-hPPARα (Figure 5C) such that the final concentration was 700 ng for each plasmid. Plasmids were first combined in microcentrifuge tubes with 100 µl serum free media and 100 µl of Lipofectamine 2000. The tubes were allowed to incubate at room temperature for 30 minutes before being added to the cover slips. Following transfection, the cells were incubated at 37°C for 4 hours before the addition of ligands. Prior to adding ligands, the media was changed to serum free so that ligand absorption could be claimed with high efficacy. All ligands were re-suspended in 50% DMSO and used at a concentration of 10µM. Ligands used for this

study include ciprofibrate, fluorobexarotene and T-0901317. After the addition of ligands, the cells were incubated at 37°C over night (18-20 hours). Based on experimental setup, visualization of the color Venus (yellow fluorescent protein, YFP) indicated the presence of the heterodimer hPPAR α -hLXR α and the color Cerulean (cyan fluorescent protein, CFP) indicated the presence of hPPAR α -hRXR α .

A second set of experiments was completed where LXR α was the central partner receptor, using plasmids encoding for Venus-hPPAR α (Figure 6A), ECFP-hLXR α (Figure 6B) and Cerulean-hRXR α (Figure 5B) at volumes of 0.5 μ l, 0.52 μ l and 0.6 μ l, respectively. For this experimental set up, visualization of the color Venus (yellow fluorescent protein, YFP) indicated the presence of the heterodimer hLXR α -hPPAR α and the color Cerulean (cyan fluorescent protein, CFP) indicated the presence of hLXR α -hRXR α . Transfections were established using Lipofectamine 2000, implementing the same procedure outlined above.

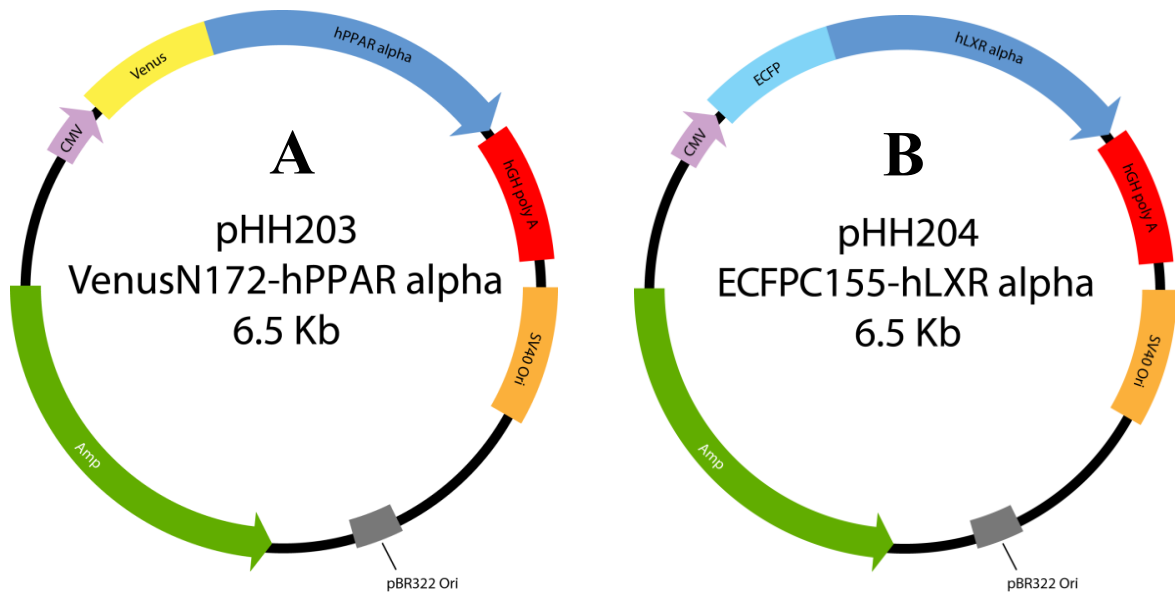


Figure 6. Schematic of plasmid DNA construction for bimolecular fluorescence complementation using transient transfections. (A) Plasmid pHH203 coding for VenusN172-hPPAR α using the ampicillin resistance gene and a CMV promoter. **(B)** Plasmid pHH204 coding for ECFPC155-hLXR α using the ampicillin resistance gene and a CMV promoter.

v. Fluorescence Microscopy

Live cells were imaged using a Zeiss confocal microscope. Sets of images were obtained via Axiovision software where exposures for CFP, YFP and DIC were set to 125 ms, 200 ms and 75 ms, respectively. Prior to imaging, cells were rinsed and replenished with fresh media (Dulbecco's Modified Eagle Medium), then allowed to incubate at 37°C for at least 10 minutes. Approximately 12-15 images were taken per coverslip in order to accurately analyze subcellular localization.

IV. RESULTS

SDS-PAGE analysis demonstrated the presence of a 50kDa protein, corresponding to full-length, recombinant proteins used in sequential experiments

All experiments in this project incorporated the use of full-length recombinant human proteins, hLXR α , hPPAR α and hRXR α , purified by affinity chromatography. After purification, all proteins were run separately on a 12% SDS-PAGE gel, indicating bands corresponding to the appropriate sizes of each nuclear receptor. Accordingly, each gel indicates the presence of full-length hPPAR α (Figure 7A), hRXR α (Figure 7B) and hLXR α (Figure 7C – provided by Shimpi Bedi) around 50kDa, consistent with the molecular weight of each protein, 52636.5Da, 51521.0Da, and 50807.2Da respectively. Furthermore, hLXR α was used in combination with hRXR α and hPPAR α to study effects of synthetic ligands, particularly evaluating the heterodimer hLXR α -hPPAR α . All proteins were concentrated in either PBS or HEPES buffer where salt concentrations were 163.7mM and 270mM, respectively.

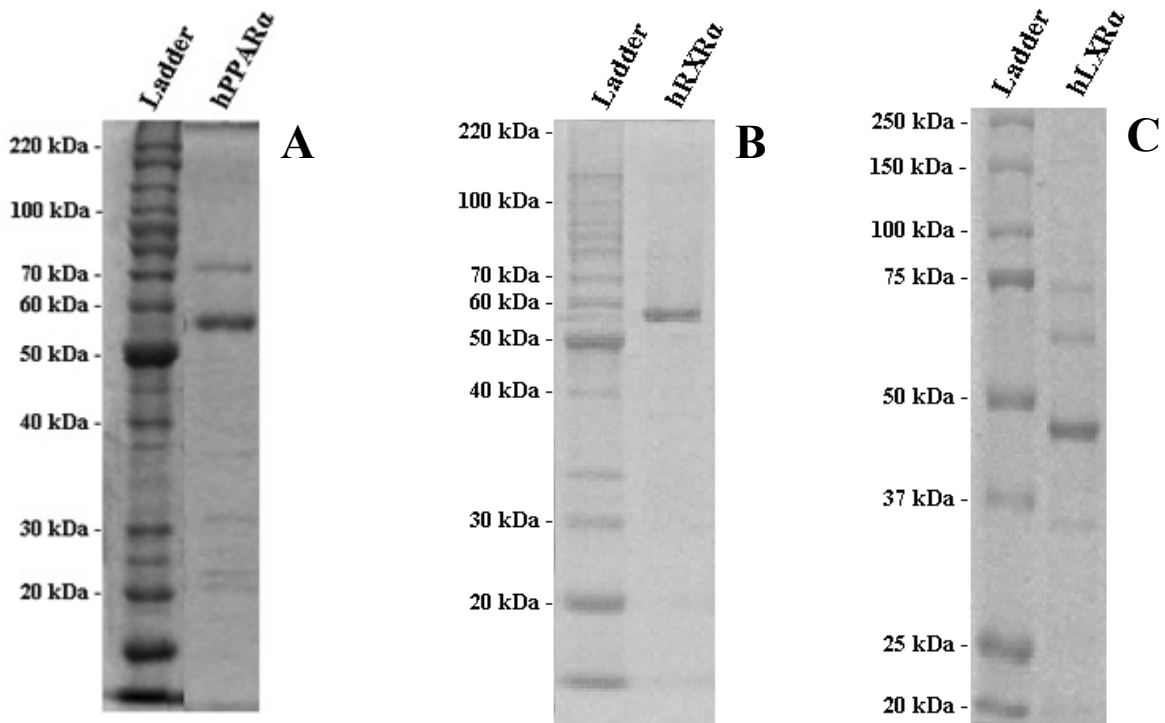


Figure 7. SDS-PAGE showing purified, full-length hPPAR α , hRXR α and hLXR α (A) 12% SDS gel indicating hPPAR α , where the 52kDa band corresponds with full-length protein, purified by affinity chromatography using a GST affinity column. Coomassie blue staining was used to stain the gel, while 7.5% acetic acid was used for de-staining. **(B)** 12% SDS gel indicating hRXR α , where the 51kDa band corresponds with full-length protein, purified by affinity chromatography using a GST affinity column. Coomassie blue staining was used to stain the gel, while 7.5% acetic acid was used for de-staining. **(C)** 12% SDS gel indicating hLXR α , where the 50kDa band corresponds with full-length protein, purified by affinity chromatography using a GST affinity column. Coomassie blue staining was used to stain the gel, while 7.5% acetic acid was used for de-staining.

* hLXR α gel image courtesy of Mrs. Shimpi Bedi, PhD Candidate

Intrinsic fluorescence quenching assays demonstrate ligand binding is not exclusive

Ligand binding may not be exclusive in terms of previously known agonistic/antagonistic properties. Each nuclear receptor (hLXR α , hPPAR α , hRXR α) was individually titrated with increasing amounts of synthetic ligand up to 300nM. Binding affinities were determined using a one-site saturation, ligand binding template on Sigma Plot©, where it was determined that each ligand binds with high affinity (K_d values in the nanomolar range). Extensive analysis was completed for all eight synthetic compounds with each nuclear receptor (LXR α , RXR α and PPAR α) individually. Even though some compounds were previously defined as agonists/antagonists for certain proteins, evaluation of each ligand with each nuclear receptor was critical to ascertain ligand exclusivity. This is novel data since ligand targets are often taken for granted without regards to the non-exclusive nature of these compounds. These assumptions are a serious concern for pharmacological development since metabolic targets are not exclusive.

Compounds such as auraptene, UVI 3003, GW-6471 and lovastatin exclusively bind their respective targets as shown with intrinsic fluorescence quenching (Figure 8). However, results indicated that some compounds do not exclusively target one nuclear receptor as previously assumed (Figures 8 and 9). In the case of fluorobexarotene, a known RXR agonist, it would seem that this compound preferentially binds hPPAR α with a higher affinity than hRXR α (Figure 9E and 9F). Similar results are seen with pravastatin, classified as a hPPAR α agonist, where binding is seen for hPPAR α as well as hRXR α (Figure 8H and 8I). This becomes therapeutically significant when treating patients with atherosclerosis and

diabetes since a given drug could have more than one target, resulting in adverse side effects. Furthermore, many drugs are often pulled from the market due to negative side effects, potentially due to numerous, unexpected nuclear receptor targets.

To further evaluate protein-ligand interactions, three ligands were selected for further assays with the hPPAR α -hLXR α heterodimer. Fluorobexarotene was chosen due to its promiscuous binding to hRXR α and hPPAR α , allowing for possible effects on both the hPPAR α -hLXR α and hRXR α -hLXR α heterodimers. Ciprofibrate was also chosen for further assays to evaluate the response of a hPPAR α agonist on the hPPAR α -hLXR α heterodimer, where this ligand exclusively acts through hPPAR α (Figure 9A-C). Lastly, compound T-0901317 was chosen as an exclusive hLXR α agonist, applicable for further assays with the hPPAR α -hLXR α heterodimer (Figure 9G-I). In all cases, protein-ligand interactions are indicative of a single binding site based on double reciprocal plots.

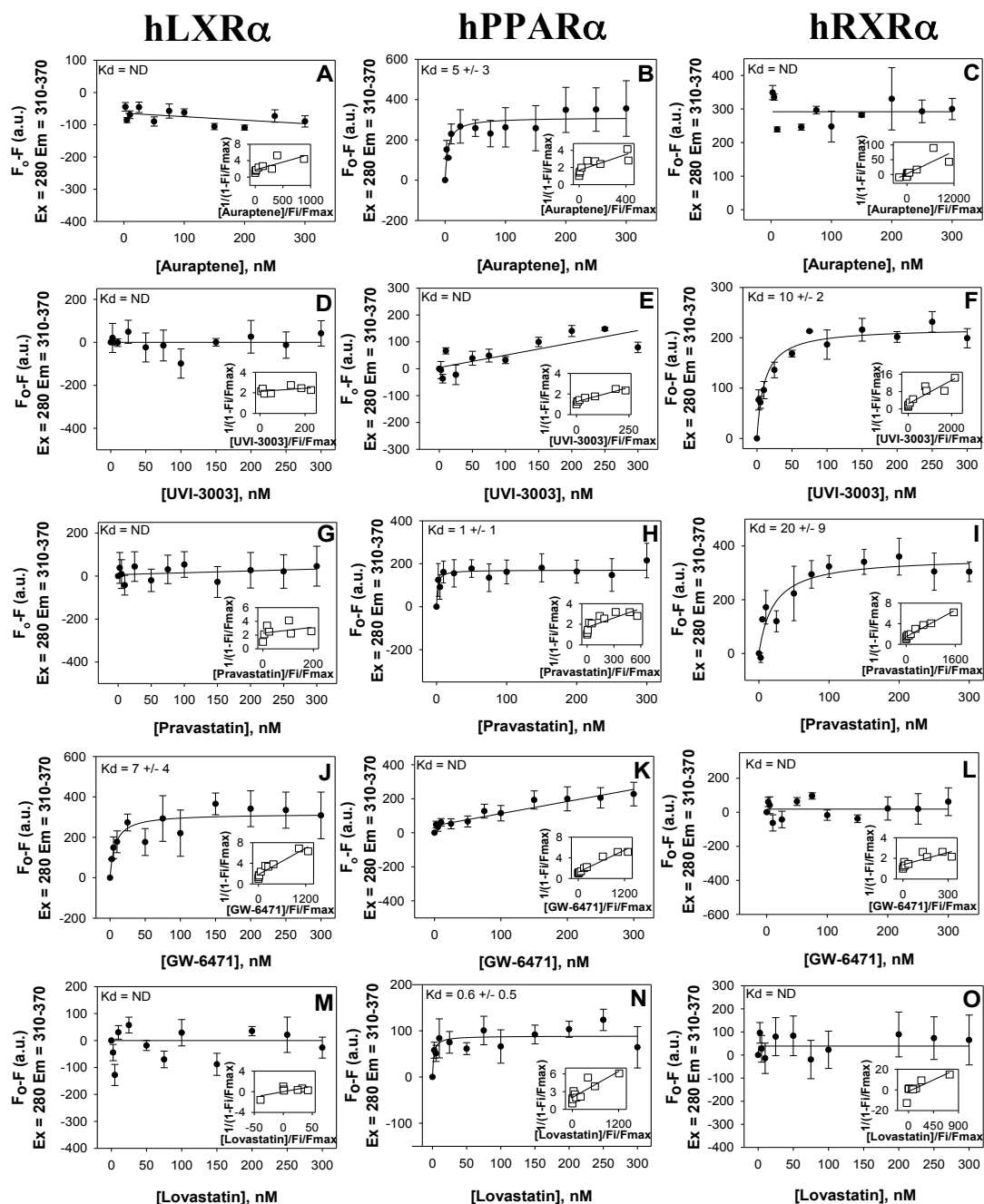


Figure 8. Intrinsic fluorescence quenching of hLXR α , hPPAR α and hRXR α with synthetic ligands used in further assays. (A-C) 100nM hLXR α , hPPAR α and hRXR α , respectively, titrated against increasing concentrations of 0nM to 300nM auraptene. **(D-F)** 100nM hLXR α , hPPAR α and hRXR α , respectively, titrated against increasing concentrations of 0nM to 300nM UVI-3003. **(G-I)** 100nM hLXR α , hPPAR α and hRXR α , respectively, titrated against increasing concentrations of 0nM to 300nM pravastatin. **(J-L)** 100nM hLXR α , hPPAR α and hRXR α , respectively, titrated against increasing concentrations of 0nM to 300nM GW-6471. **(M-O)** 100nM hLXR α , hPPAR α and hRXR α , respectively, titrated against increasing concentrations of 0nM to 300nM lovastatin. The x-axis represents ligand concentration and the y-axis represents the change in fluorescence intensity for all plots.

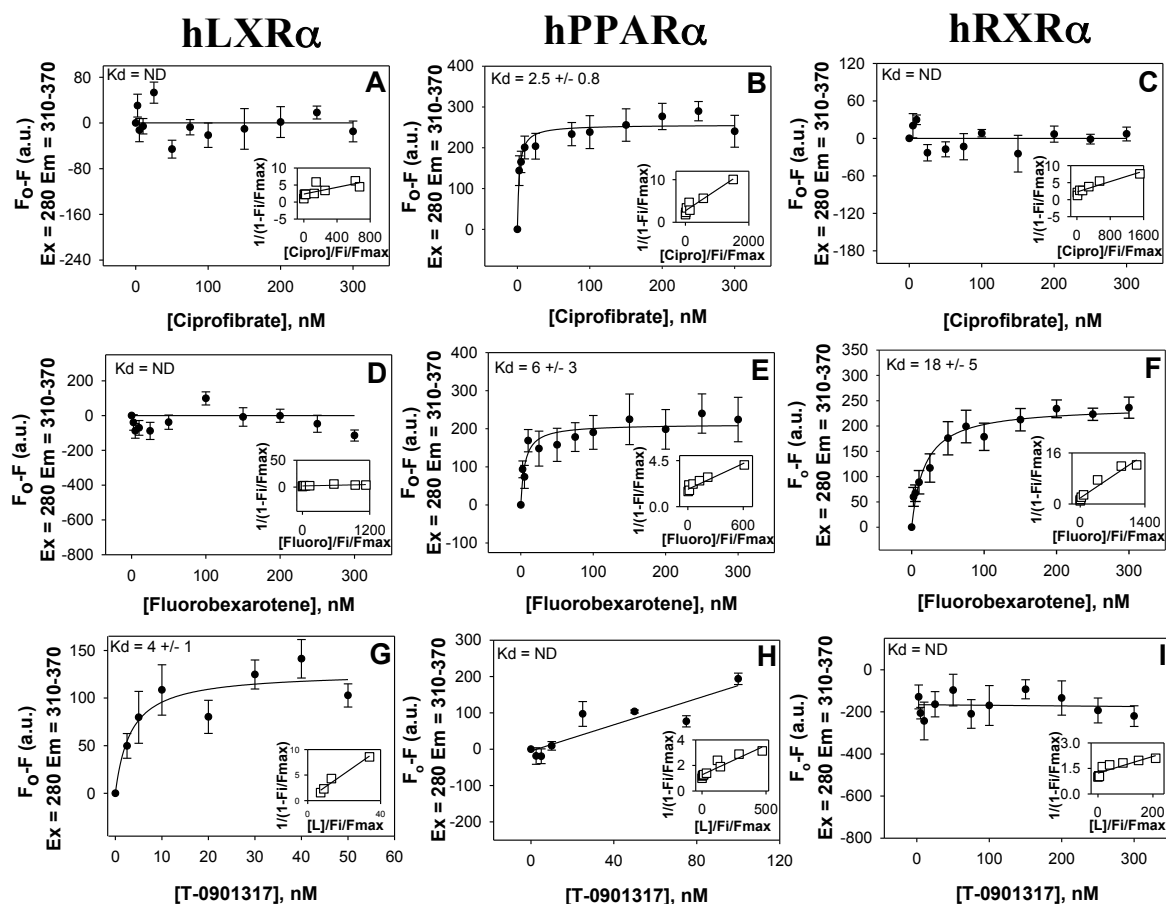


Figure 9. Intrinsic fluorescence quenching of hLXR α , hPPAR α and hRXR α with synthetic ligands used in further assays. (A-C) 100nM hLXR α , hPPAR α and hRXR α , respectively, titrated against increasing concentrations of 0nM to 300nM ciprofibrate. The x-axis represents ciprofibrate concentration and the y-axis represents the change in fluorescence intensity. **(D-F)** 100nM hLXR α , hPPAR α and hRXR α , respectively, titrated against increasing concentrations of 0nM to 300nM fluorobexarotene. The x-axis represents fluorobexarotene concentration and the y-axis represents the change in fluorescence intensity. **(G-I)** 100nM hLXR α , hPPAR α and hRXR α , respectively, titrated against increasing concentrations of 0nM to 300nM T-0901317. The x-axis represents T-0901317 concentration and the y-axis represents the change in fluorescence intensity. Insets represent double reciprocal plots of each binding assay.

Table 2. Intrinsic fluorescence quenching of 100nM hLXR α , hPPAR α and hRXR α titrated with synthetic ligands (100 μ M).

Synthetic Compound	Kd (hLXRα) (nM)	Kd (hPPARα) (nM)	Kd (hRXRα) (nM)
Ciprofibrate	ND	2.5 \pm 0.8	ND
Fluorobexarotene	ND	6.0 \pm 3.0	18.0 \pm 5.0
T-0901317	4.0 \pm 1.0	ND	ND

ND = Not determinable

Synthetic ligands induce changes in the secondary structure of the hPPAR α -hLXR α heterodimer

Circular dichroism was used to visualize changes in secondary structure of the novel heterodimer hLXR α -hPPAR α in response to synthetic ligands. This technique utilizes left and right circularly polarized light to generate differential absorption spectra. The circular dichroism experiment required the use of full-length hPPAR α and hLXR α , in addition to synthetic ligands solubilized in DMSO or ethanol at a concentration of 5 μ M.

Characteristically, in the absence of ligand, the circular dichroic spectra of hLXR α -hPPAR α demonstrates a positive peak around 190nm and two negative peaks around 210-220nm (Figure 10). Accordingly, this is indicative of an alpha-helical structure, consistent with previous data [29]. When ciprofibrate and fluorobexarotene are introduced, the spectra become slightly distorted, reducing the estimate of alpha helical content (Figure 10A and 10B). This finding was confirmed upon computational and statistical analysis of percent composition regarding regular and distorted α -helices, β -sheets, turns and unordered structures using Sigma Plot $\text{\textcircled{C}}$. Fluorobexarotene induced conformational changes in the secondary structure of hLXR α -hPPAR α , particularly regarding turns where the p value was <0.06 (Table 3). Ciprofibrate demonstrated variations in the estimated α -helices and turns of the hLXR α -hPPAR α heterodimer where p values were <0.0001 and <0.01, respectively (Table 3). On the other hand, it would appear T-0901317 induces conformational changes consistent with an increase in estimated alpha-helical content (Figure 10C). This result was further confirmed by structural analysis where both regular and distorted α -helices, β -sheets and turns yielded p values of <0.0001 (Table 3),

suggesting T-0901317 has a significant effect on the secondary structure of hLXR α -hPPAR α . This would indicate that these synthetic ligands could significantly alter secondary structure of the heterodimer hLXR α -hPPAR α , as a whole, potentially affecting unforeseen metabolic targets in therapeutic medicine.

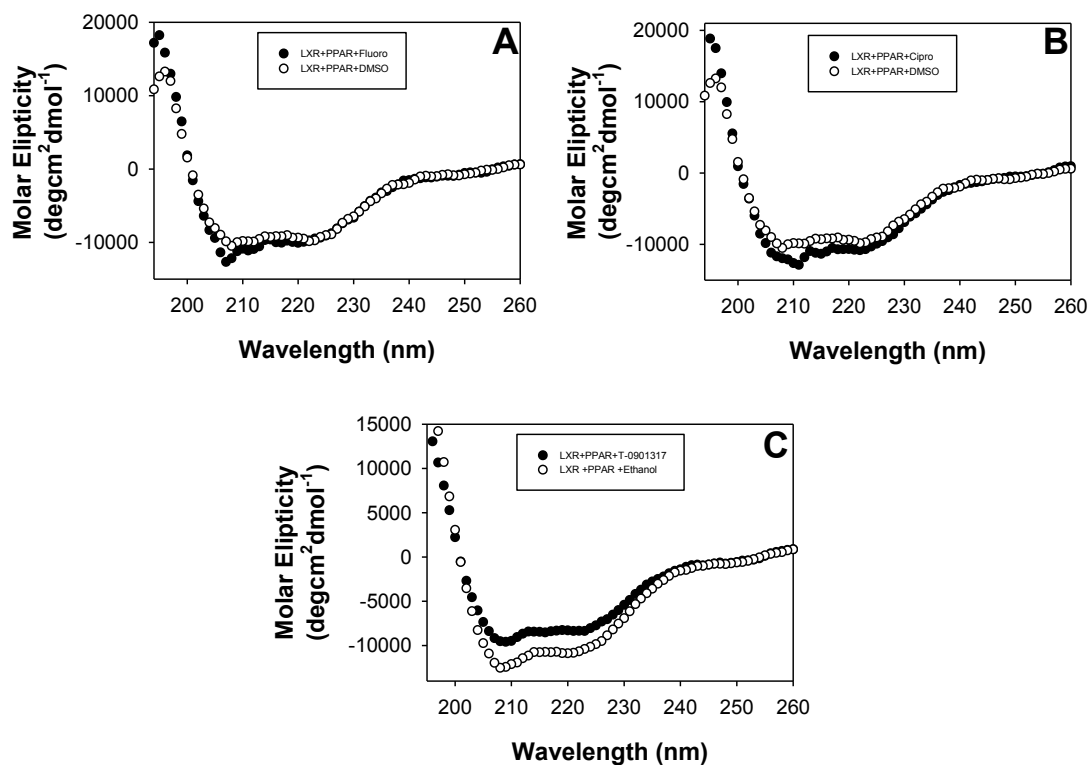


Figure 10. Circular Dichroic spectra of a mixture of hPPAR α and hLXR α in the presence and absence of synthetic ligands. (A) Far-UV spectra of a mixture of equal amino acid molarities of hPPAR α and hLXR α in the absence (open circles) and presence (closed circles) of 5 μ M fluorobexarotene. **(B)** Far-UV spectra of a mixture of equal amino acid molarities of hPPAR α and hLXR α in the absence (open circles) and presence (closed circles) of 5 μ M ciprofibrate. **(C)** Far-UV spectra of a mixture of equal amino acid molarities of hPPAR α and hLXR α in the absence (closed circles) and presence (open circles) of 5 μ M T-0901317. Each spectrum is composed of an average of ten scans, taken from three replicates. Fluoro – fluorobexarotene, Cipro - ciprofibrate

Table 3. Secondary structures of hPPAR α and hLXR α (corrected for solvent effect) in the presence and absence of synthetic ligands

Ligand	α -helix	α -helix	β -sheet	β -sheet	Turns	Unrd
	regular H(r) %	distorted H(d) %	regular S(r) %	distorted S(d) %	T %	U %
DMSO	24.5 \pm 0.5	20.5 \pm 3.5	12.0 \pm 2.0	14.5 \pm 0.5	11.5 \pm 0.5	16.5 \pm 0.5
Ethanol	21.4 \pm 0.6	14.9 \pm 0.4	8.5 \pm 0.2	6.9 \pm 0.1	17.1 \pm 0.2	31.3 \pm 0.8
Fluorobexarotene	23.3 \pm 1.3	21.3 \pm 1.5	12.0 \pm 1.1	15.3 \pm 0.3	14.3 \pm 0.7*	15.0 \pm 1.5
Ciprofibrate	20.7 \pm 0.7***	19.3 \pm 0.9	13.3 \pm 1.2	16.0 \pm 0.6	17.0 \pm 0.6**	14.0 \pm 1.0
T-0901317	15.6 \pm 0.8***	12.6 \pm 0.3***	11.5 \pm 0.7***	8.4 \pm 0.3***	20.1 \pm 0.2***	31.8 \pm 0.5

Asterisks (*) represent significant differences due to presence of ligand as compared with the absence of ligand for all panels. *p = <0.06, **p = <0.01, ***p = <0.0001.

Alexa Fluor dyes 488 and 555 are optimal for fluorescence resonance energy transfer (FRET) experiments

Fluorescence resonance energy transfer allows for the visualization of energy transfer between two fluorescently labeled molecules. This experiment utilizes Alexa Fluor (AF) dyes, as opposed to Cy3 and Cy5 dyes, due to enhanced environmental stability. Even so, certain dye-protein combinations may not be favorable in terms of FRET. Ideally, the chosen fluorophore would yield minimal changes in fluorescence when titrated with the unlabeled molecule of interest. Confirmation of this phenomenon required preliminary tests where each protein was labeled with a certain Alexa Fluor dye and titrated with an unlabeled partner receptor.

Based on experimental results, hPPAR α labeled with AF-555 was an ideal dye-protein combination for FRET, where hRXR α was the partner receptor (Figure 11A). When AF-555hPPAR α was titrated against unlabeled hRXR α there were minimal changes in fluorescence, suggesting AF-555hPPAR α is a useful candidate for FRET. While this dye-protein combination seems promising, the novel heterodimer hPPAR α -hLXR α is the point of interest. The same preliminary experiment was completed for AF-555hPPAR α titrated against unlabeled hLXR α , yet this yielded changes in fluorescence upon dimerization (Figure 11B). Similar experiments were implemented for AF-555hRXR α , however, changes in fluorescence were visualized upon dimerization with both hLXR α and hRXR α (Figure 11C and 11D). Since AF-555hPPAR α showed the most environmental stability when titrated against unlabeled hRXR α , this dye-protein combination is favorable for FRET.

Similarly, spectra for AF-488hLXR α , titrated with increasing amounts of either unlabeled hRXR α or hPPAR α (Figure 12A and 12B), demonstrated a minimal change in fluorescence, suggesting AF-488hLXR α is an ideal dye-protein combination for further FRET experiments. Alexa Fluor 488-hPPAR α would also be an acceptable dye-protein combination since changes in fluorescence were minimal (Figure 12C and 12D). However, when Alexa Fluor dye 488 was used to label hRXR α , changes in fluorescence were visualized upon titration against unlabeled partner receptors, suggesting AF-488hRXR α is not optimal for FRET (Figure 12E and 12F).

Lastly, Alexa Fluor dye 594 was examined in a similar fashion where AF-594hRXR α was titrated against unlabeled hLXR α and hPPAR α (Figure 13A and 13B, respectively). Unfortunately, changes in fluorescence were visualized upon dimerization, indicating Alexa Fluor dye 594 may be problematic for FRET. The nature of extrinsic fluorophores is not concrete and environmental stability may still be a factor. Based on experimental results and available resources, AF-488hLXR α was chosen as the donor and AF-555hPPAR α was chosen as the acceptor for further FRET experiments.

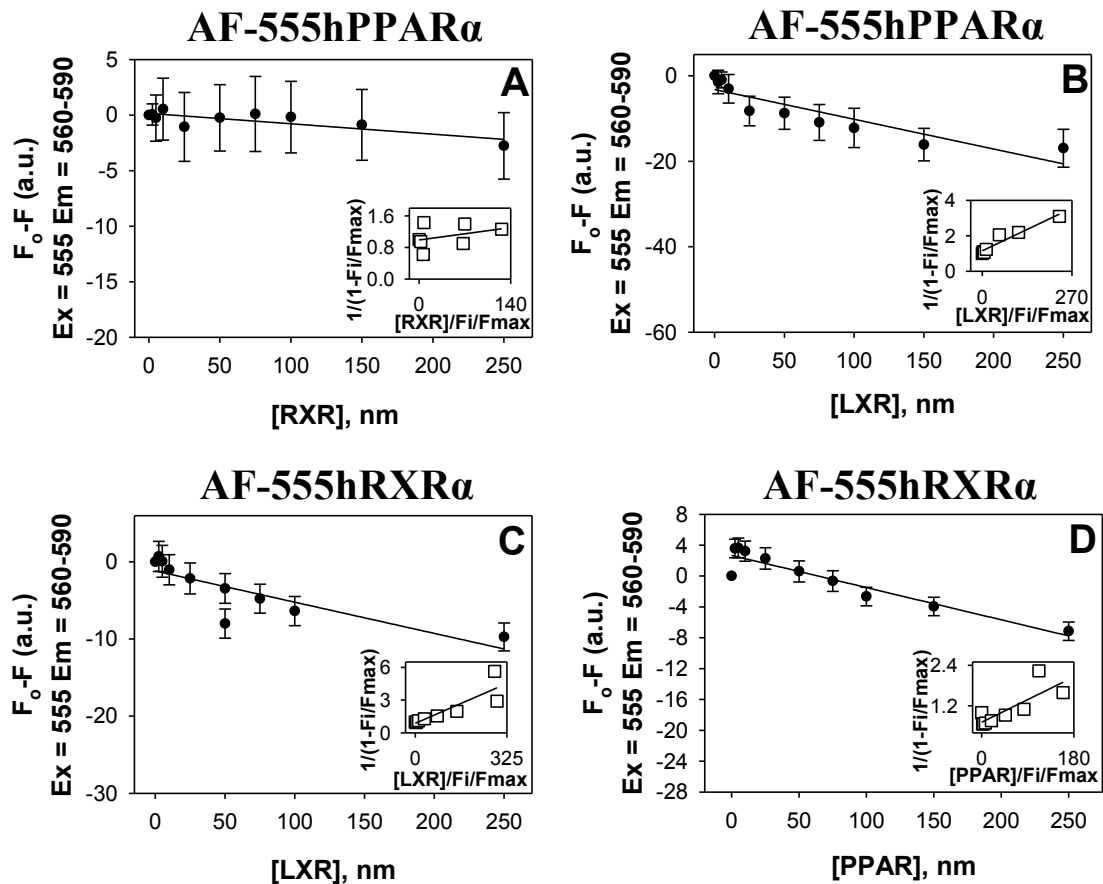


Figure 11. Fluorescent binding assays using Alexa Fluor (AF) 555-labeled protein, titrated against increasing concentrations of unlabeled protein. (A) 25nM of AF-555hPPAR α was titrated against increasing concentrations of 0nM to 250nM hRXR α . The x-axis indicates the concentration of the titrant, hRXR α , while the y-axis represents changes in fluorescence intensity. (B) 25nM of AF-555hPPAR α was titrated against increasing concentrations of 0nM to 250nM hLXR α . The x-axis indicates the concentration of hLXR α , while the y-axis represents changes in fluorescence intensity. (C) 25nM of AF-555hRXR α was titrated against increasing concentrations of 0nM to 250nM hLXR α . The x-axis indicates the concentration of hLXR α , while the y-axis represents changes in fluorescence intensity. (D) 25nM of AF-555hRXR α was titrated against increasing concentrations of 0nM to 250nM hPPAR α . The x-axis indicates the concentration of hPPAR α , while the y-axis represents changes in fluorescence intensity. Insets represent double reciprocal plots.

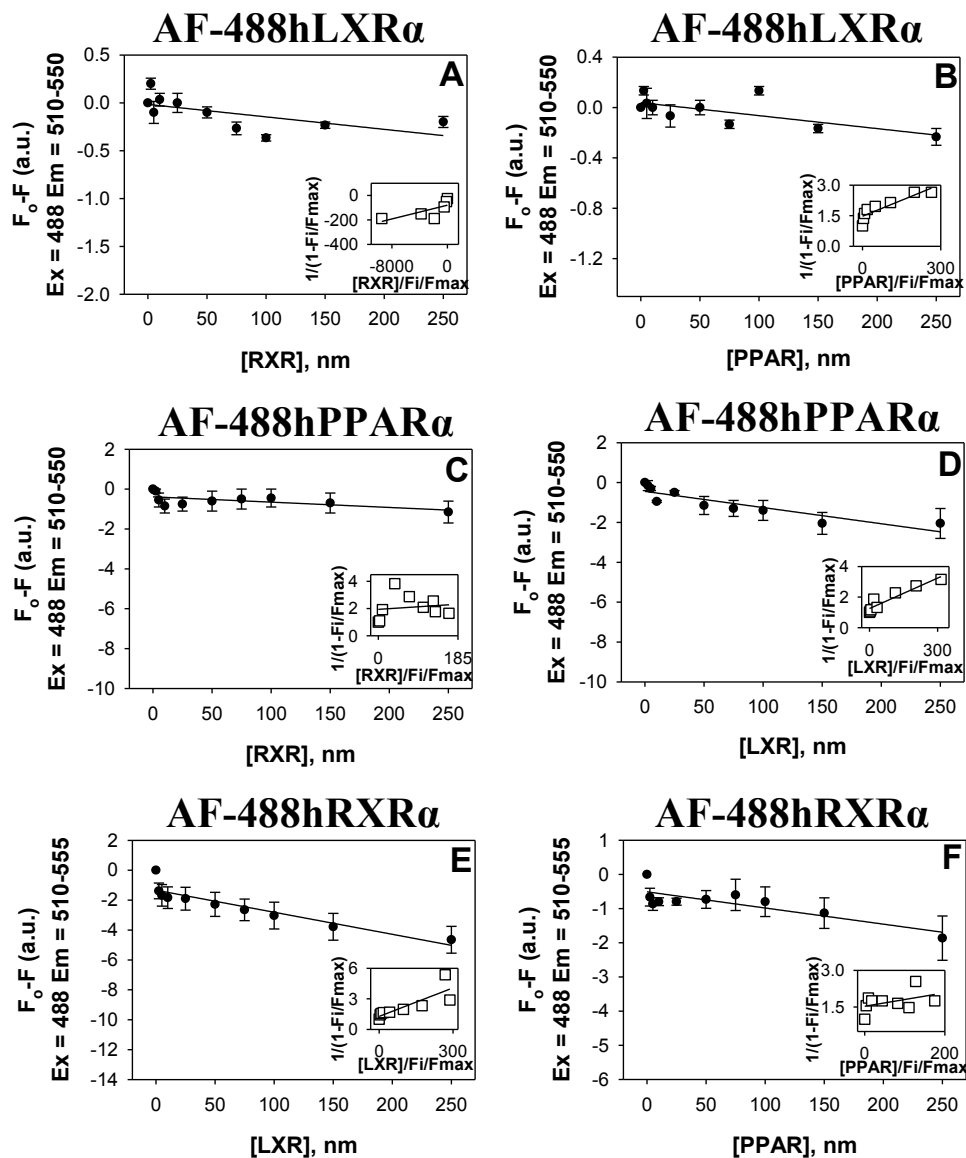


Figure 12. Fluorescent binding assays using Alexa Fluor (AF) 488-labeled protein, titrated against increasing concentrations of unlabeled protein. (A) 25nM of AF-488hLXR α was titrated against increasing concentrations of 0nM to 250nM hRXR α . The x-axis indicates the concentration of the titrant, hRXR α , while the y-axis represents changes in fluorescence intensity. (B) 25nM of AF-488hLXR α was titrated against increasing concentrations of 0nM to 250nM hPPAR α . The x-axis indicates the concentration of hPPAR α , while the y-axis represents changes in fluorescence intensity. (C) 25nM of AF-488hPPAR α was titrated against increasing concentrations of 0nM to 250nM hRXR α . The x-axis indicates the concentration of hRXR α , while the y-axis represents changes in fluorescence intensity. (D) 25nM of AF-488hPPAR α was titrated against increasing concentrations of 0nM to 250nM hLXR α . The x-axis indicates the concentration of hLXR α , while the y-axis represents changes in fluorescence intensity. (E) 25nM of AF-488hRXR α was titrated against increasing concentrations of 0nM to 250nM hLXR α . The x-axis indicates the concentration of hLXR α , while the y-axis represents changes in fluorescence intensity. (F) 25nM of AF-488hRXR α was titrated against increasing concentrations of 0nM to 250nM hPPAR α . The x-axis indicates the concentration of hPPAR α , while the y-axis represents changes in fluorescence intensity. Insets represent double reciprocal plots.

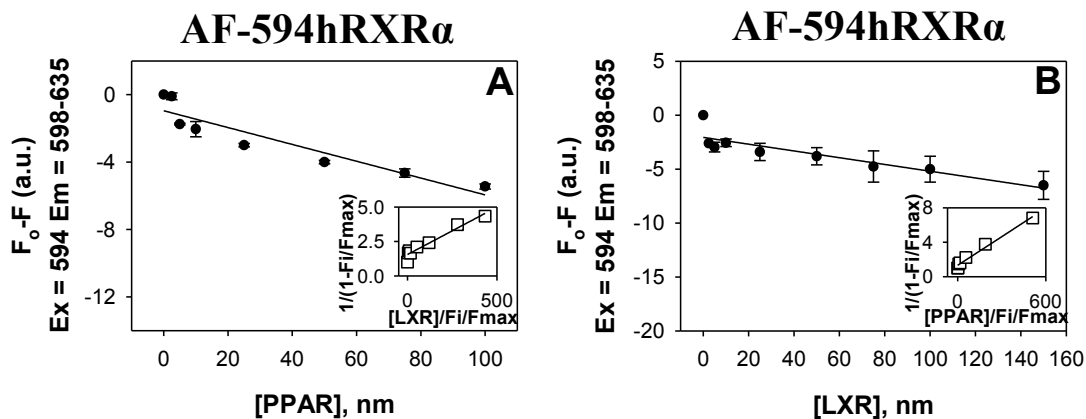


Figure 13. Fluorescent binding assays using Alexa Fluor (AF) 594-labeled protein, titrated against increasing concentrations of unlabeled protein. (A) 25nM of AF-594hRXR α was titrated against increasing concentrations of 0nM to 150nM hLXR α . The x-axis indicates the concentration of the titrant, hLXR α , while the y-axis represents changes in fluorescence intensity. **(B)** 25nM of AF-594hRXR α was titrated against increasing concentrations of 0nM to 150nM hPPAR α . The x-axis indicates the concentration of hPPAR α , while the y-axis represents changes in fluorescence intensity.

Nuclear receptors hPPAR α and hLXR α bind with high affinity, as shown by FRET

Characteristically, when two proteins dimerize, energy transfer can be visualized via FRET where there is a decrease in donor emission, with a concomitant increase in acceptor emission when excited at the proper wavelength. When AF-488hLXR α is titrated against AF-555hPPAR α , the raw spectrum depicts the occurrence of FRET, indicated by a decrease in donor emission around 520nm and an increase in acceptor emission around 565nm (Figure 14A). Either the donor or acceptor peaks can be used to generate a binding curve where binding affinity can be quantified. Based on this quantitative assay using peak values from quenching, hPPAR α and hLXR α exhibit a binding affinity of 8 ± 3 nM (Figure 14B). Biological effects of this novel heterodimer are still being studied, however, knowledge of this interaction could benefit diseases such as atherosclerosis and diabetes. In particular, effects of synthetic ligands on this heterodimer would be beneficial in demonstrating pharmacological effects on a cellular level.

A similar experiment was performed with AF-488hLXR α and AF-555hRXR α to verify that this technique is effective. Subsequently, FRET was observed via a decrease in donor emission around 520nm and an increase in acceptor emission around 565nm (Supplemental Figure 2A). A binding curve was generated from the emission data, confirming hLXR α and hRXR α bind with high affinity (Supplemental Figure 2B). This solidifies the knowledge that FRET is an accurate measure of affinity with regards to nuclear receptors.

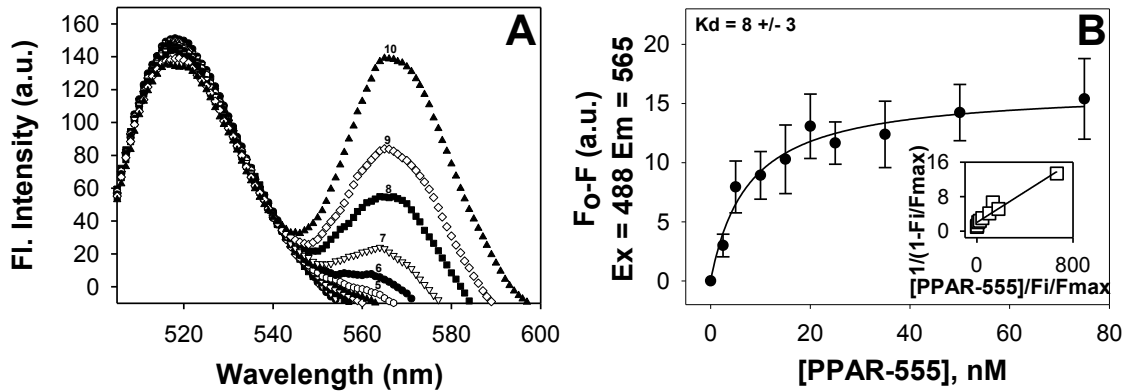


Figure 14. FRET using AF-488hLXR α as the donor and AF-555hPPAR α as the acceptor.

(A) 25nM AF-488hLXR α titrated against increasing concentrations of 0nM to 100nM AF-555hPPAR α . The x-axis represents wavelength (nm) and the y-axis depicts fluorescence intensity. Excitation wavelength was set at 488nm and emission scans were collected over a range of 500-667nm. **(B)** 25nM AF-488hLXR α titrated against increasing concentrations of 0nM to 100nM AF-555hPPAR α . The x-axis indicates the concentration of AF-555hPPAR α and the y-axis represents changes in fluorescence intensity.

Synthetic ligands have an effect on the binding affinity of hLXR α and hPPAR α

The effects of synthetic ligands on the novel heterodimer, hLXR α -hPPAR α , could provide valuable insight into therapeutic medicine. Cholesterol and diabetic drugs are often pulled from the market due to increasingly negative side effects in humans. The hLXR α -hPPAR α heterodimer is a key component of cholesterol homeostasis and metabolic pathways, where knowledge of cellular interactions could provide valuable insight to therapeutic medicine. Fluorescence resonance energy transfer experiments demonstrate ciprofibrate and T-0901317 increase the K_d value of the hLXR α -hPPAR α heterodimer to $11 \pm 2\text{nM}$ and $10 \pm 2\text{nM}$, respectively (Figure 15A and 15B). When similar energy transfer experiments were done with fluorobexarotene, the K_d value decreased to $5 \pm 1\text{nM}$ (Figure 15C), suggesting fluorobexarotene enhances the binding affinity between hLXR α and hPPAR α . This data may be therapeutically significant since a known RXR agonist induces a change in dimerization of hLXR α -hPPAR α , possibly providing an explanation for negative side effects, such as increased triglycerides, often associated with cholesterol and diabetes medications.

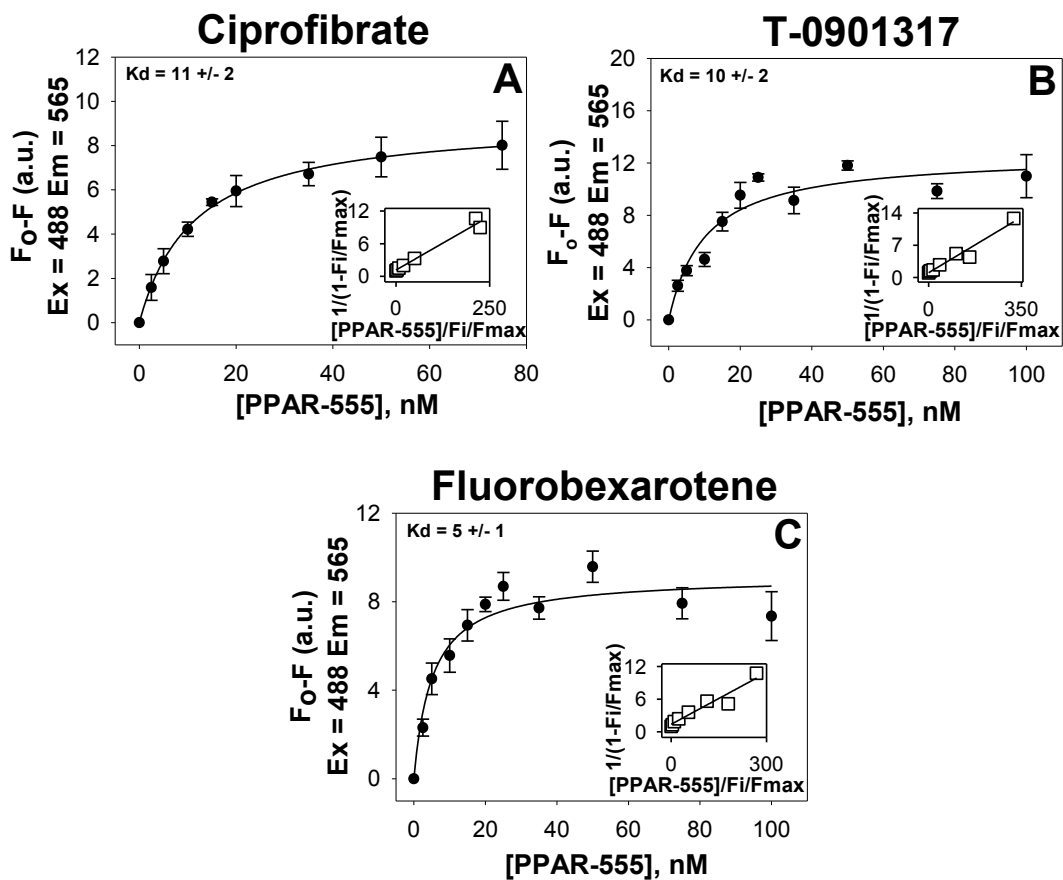


Figure 15. FRET using AF-488hLXR α as the donor and AF-555hPPAR α as the acceptor in the presence of synthetic ligands. (A) 25nM AF-488hLXR α titrated against increasing concentrations of 0nM to 75nM AF-555hPPAR α in the presence of 6nM ciprofibrate. The x-axis indicates the concentration of AF-555hPPAR α and the y-axis represents changes in fluorescence intensity. (B) 25nM AF-488hLXR α titrated against increasing concentrations of 0nM to 100nM AF-555hPPAR α in the presence of 10nM T-0901317. The x-axis indicates the concentration of AF-555hPPAR α and the y-axis represents changes in fluorescence intensity. (C) 25nM AF-488hLXR α titrated against increasing concentrations of 0nM to 100nM AF-555hPPAR α in the presence of 13nM fluorobexarotene. The x-axis indicates the concentration of AF-555hPPAR α and the y-axis represents changes in fluorescence intensity.

Table 4. Fluorescence resonance energy transfer of 25nM AF-488hLXR α titrated against AF-555hPPAR α over a range of 0nM to 100nM in the presence and absence of synthetic ligands.

Synthetic Compound	Kd (hLXRα-hPPARα) (nM)
No ligand	8 \pm 3
Ciprofibrate	11 \pm 2
Fluorobexarotene	5 \pm 1
T-0901317	10 \pm 2

Stably transfected COS-7 cells contain all three nuclear receptor plasmids, as shown with PCR testing

Stable COS-7 BiFC clones were analyzed via PCR to verify the presence of all three nuclear receptor plasmids. Stable COS-7 cells used in this project were engineered by Heather Hostetler, PhD and S. Dean Rider, Jr., PhD. The original goal was to verify the presence of all three nuclear receptors in these cells before treating with synthetic ligands. It is possible that some COS-7 clones created in this fashion, did not integrate and express all three nuclear receptors. Therefore, it was important to solidify the presence of all plasmids to ensure that future effects seen with synthetic ligands were valid.

Initially, the use of stably transfected cells were preferable because it would be possible to ensure complete integration of the appropriate nuclear receptor into the cell's genome, where genetic information would be passed on to future generations. Accordingly, effects seen by an added nutrient or ligand would be uncontested. Out of 49 COS-7 clones analyzed, 15 indicated successful integration of all three proteins and were further used in fluorescence microscopy studies (Figure 16).

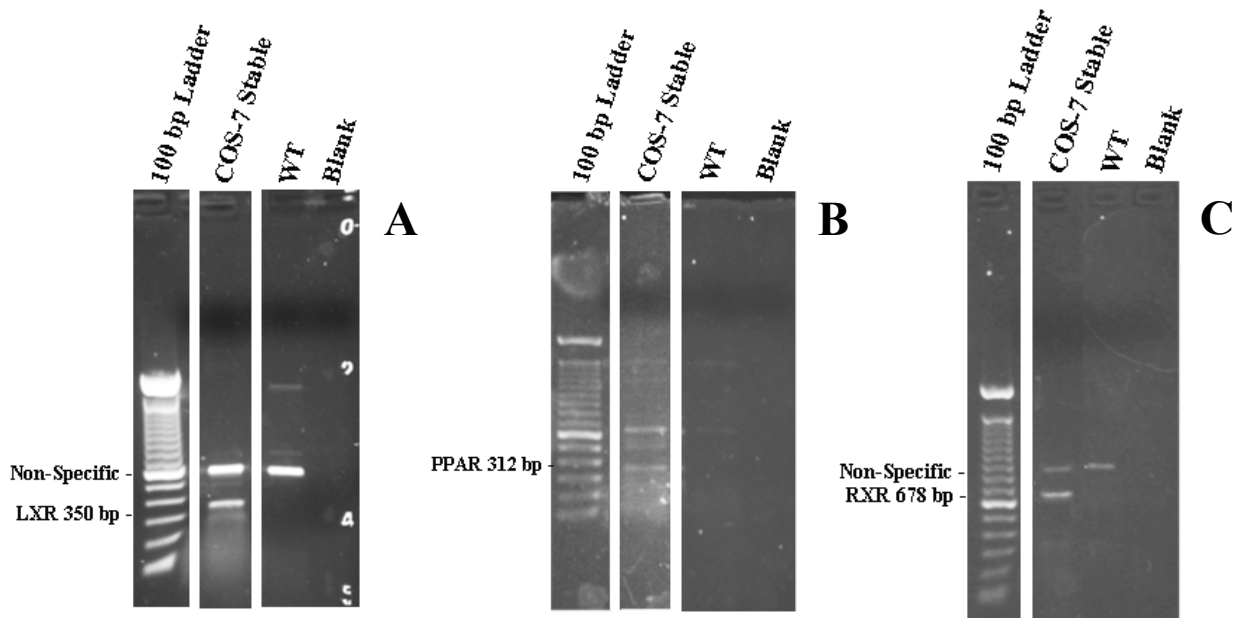


Figure 16. Electrophoresis showing the presence of nuclear receptor plasmids in COS-7, stably transfected cells. (A) 1% agarose gel showing the presence of the hLXR α plasmid (350 base pairs), isolated by DNA chloroform extraction and evaluated using PCR. (B) 1% agarose gel showing the presence of the hPPAR α plasmid (312 base pairs), isolated by DNA chloroform extraction and evaluated by PCR. (C) 1% agarose gel showing the presence of the hRXR α plasmid (678 base pairs), isolated by DNA chloroform extraction and evaluated by PCR.

WT – wild type COS-7 cells (no transfection), bp – base pairs, PCR – polymerase chain reaction

BiFC quantitative analysis indicates variation in subcellular localization of transiently transfected COS-7 cells, in response to synthetic ligands

Fluorescence microscopy was utilized to visualize changes in fluorescence intensity and subcellular localization in COS-7 cells. Initially, stably transfected cells were utilized to ensure the presence of all three nuclear receptors before the addition of ligands. Fluorescence microscopy was used to analyze these cells in the absence of ligand to ascertain a baseline for sequential experiments, where ligands would be tested for their ability to alter heterodimer formation. Ideally, transfected cells would exhibit nuclear fluorescence, with an absence of fluorescence seen in un-transfected COS-7 cells. Resulting fluorescent images that were obtained from the stably transfected cells were difficult to analyze due to punctuate fluorescence in both CFP and YFP (Figure 17). This anomaly could be attributed to variations dependent on cell cycle. As a result, quantitative analysis was unattainable for these images and future experiments employed the use of transient transfections.

Transient transfections of COS-7 cells displayed nuclear fluorescence which allowed for further quantitative analysis via ImageJ© software. Fluorescence microscopy indicated nuclear fluorescence for most of the transfected cells in the presence and absence of synthetic ligand (Figure 18). In this case, “wild type” refers to transfected cells in the absence of ligand, where resulting fluorescent images could be used as a baseline for ligand comparisons. Analysis of fluorescence intensity and co-localization were compared to wild type images to understand *in vivo* effects of synthetic ligands.

Quantitative analysis of transiently transfected COS-7 cells focused on variations in fluorescence intensity and subcellular localization. The experiment was set up such that ECFP-hPPAR α was the central receptor while Cerulean-hRXR α and Venus-hLXR α were the partner receptors. In this case, resulting fluorescent images would display hPPAR α -hLXR α interaction as yellow and hPPAR α -hRXR α interaction as cerulean (blue). Analysis of fluorescence intensity utilized numerical values, tabulated from corrected total cell fluorescence (CTCF). Results indicated nearly parallel lines when CTCF was plotted against K_d values, previously determined from FRET (Figure 19A). This would suggest fluorescence intensity is nearly the same across all experimental compounds, directing us to use overlap R for co-localization analysis. This particular variable, R, is representative of subcellular localization in the nucleus, which does not incorporate pixel averaging. Therefore, the resulting value would be between 0 and 1 and would be insensitive to intensity variations. This is preferable when compared to Pearson's coefficient, which also evaluates the extent of overlap between two images, because variations in pixel intensity would present a misleading readout. Accordingly, quantitation of nuclear co-localization yielded numerical values between 0 and 1 where wild type cells presented a R value of 0.9894, while synthetic compounds ciprofibrate, fluorobexarotene and T-0901317, yielded R values of 0.9858, 0.9899 and 0.9819, respectively (Figure 19B). While these changes are seemingly small and yield no statistical significance, the fact that changes are seen should be noted. Furthermore, it would seem that co-localization (R) shows a decreasing trend with increasing K_d values. The K_d values plotted in this fashion represent binding affinities for the

hPPAR α -hLXR α heterodimer, however, evaluation with synthetic ligands could have unanticipated effects on the hPPAR α -hRXR α heterodimer. This could be important when treating human patients with synthetic compounds since desired outcomes may not be exclusive, resulting in unforeseen side effects.

An additional experiment was completed where ECFP-hLXR α was made to be the central receptor, while the partner receptors were Cerulean-hRXR α and Venus-hPPAR α . In this case, dimerization of hLXR α -hRXR α would result in a cerulean color and hLXR α -hPPAR α would produce a yellow color. Similar analysis of fluorescence intensity and co-localization were established in sequential experiments, evaluating the presence of hLXR α -hPPAR α and hLXR α -hRXR α in the cell nucleus (Supplemental Figures 4A and 4B). The anomaly in this data is treatment with T-0901317, which can potentially affect both heterodimers, adding another layer of complication since K_d values used for co-localization plots are for hPPAR α -hLXR α . Even so, co-localization analysis in this case displays no significant changes when compared to K_d values of hLXR α -hPPAR α (Supplemental Figure 4B). It should be noted that results from this experiment are not comparable to the previous experiments where hPPAR α was the central receptor since this experiment utilizes hLXR α as the central receptor.

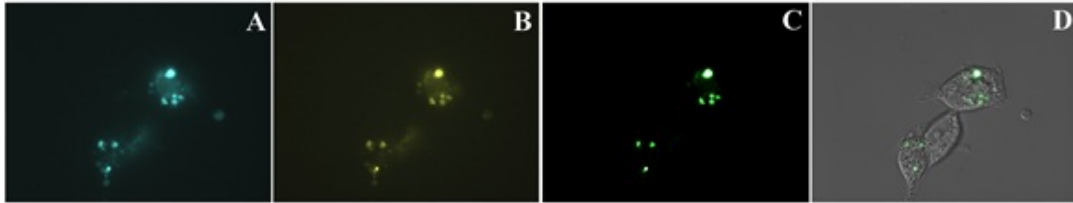


Figure 17. Fluorescence microscopy of stably transfected COS-7 cells in the absence of ligand. (A) CFP in three COS-7 cells. (B) YFP in three COS-7 cells. (C) Overlay of CFP and YFP in three COS-7 cells. (D) DIC image with an overlay of CFP and YFP in three COS-7 cells. Visualization of these cells indicates healthy growing conditions.

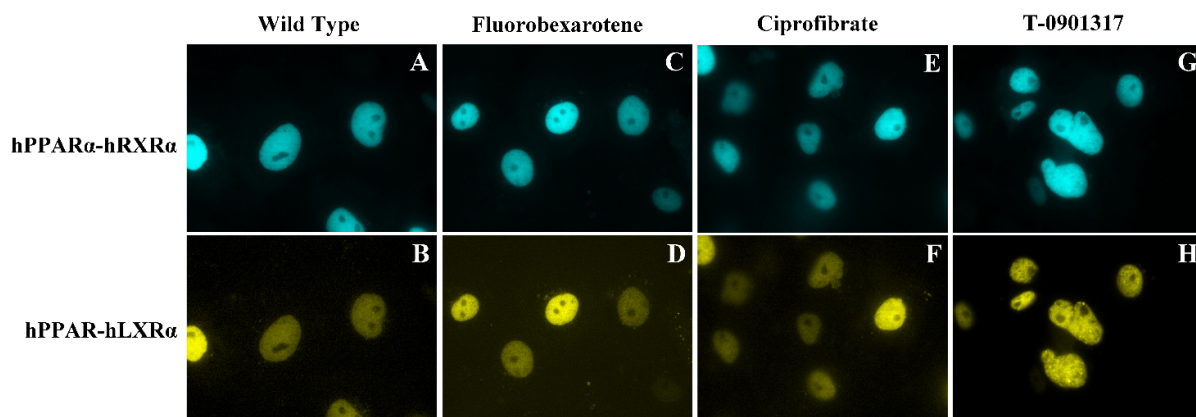


Figure 18. Fluorescence microscopy indicates nuclear fluorescence for all transiently transfected COS-7 cells, in the absence and presence of synthetic ligand. (A-B) CFP and YFP, respectively, in wild type COS-7 cells, in the absence of synthetic ligand. Cyan is indicative of hPPAR α -hRXR α and yellow is indicative of hPPAR α -hLXR α . **(C-D)** CFP and YFP, respectively, in COS-7 cells in the presence of 10 μ M fluorobexarotene. Cyan is indicative of hPPAR α -hRXR α and yellow is indicative of hPPAR α -hLXR α . **(E-F)** CFP and YFP, respectively, in COS-7 cells in the presence of 10 μ M ciprofibrate. Cyan is indicative of hPPAR α -hRXR α and yellow is indicative of hPPAR α -hLXR α . **(H-I)** CFP and YFP, respectively, in COS-7 cells in the presence of 10 μ M T-0901317. Cyan is indicative of hPPAR α -hRXR α and yellow is indicative of hPPAR α -hLXR α .

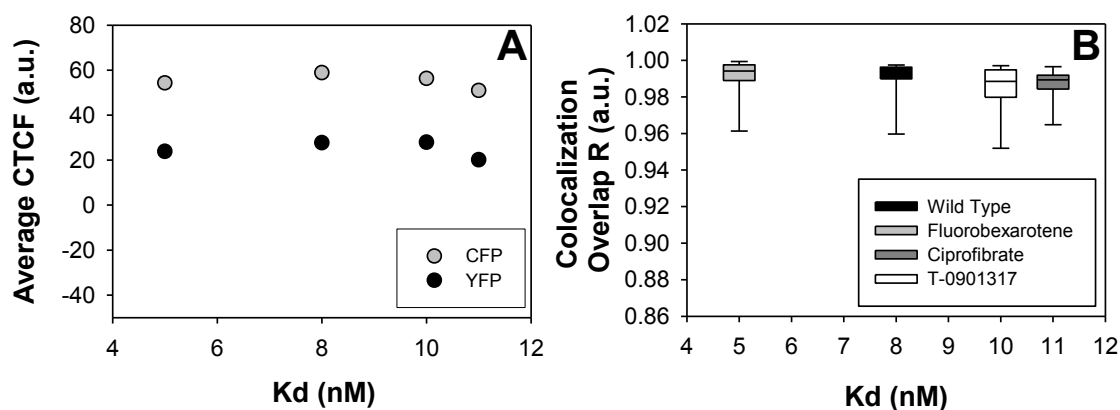


Figure 19. Quantitative analysis of transiently transfected COS-7 cells in response to synthetic ligands where ECFP-hPPAR α is the central partner receptor. (A) Fluorescence intensity for CFP and YFP in the absence and presence of synthetic ligands. The x-axis indicates K_d values for the hPPAR α -hLXR α heterodimer, previously determined from FRET in the absence and presence of ciprofibrate, fluorobexarotene and T-0901317. The y-axis indicates the average corrected total cell fluorescence (CTCF) for both CFP and YFP. (B) Co-localization of hLXR α and hPPAR α in COS-7 cell nuclei in the absence and present of synthetic ligands. The x-axis indicates K_d values for the hPPAR α -hLXR α heterodimer, previously determined from FRET in the absence and presence of ciprofibrate, fluorobexarotene and T-0901317. The y-axis indicates co-localization overlap, R, which is insensitive to variations in fluorescence intensity.

V. DISCUSSION

Diseases such as atherosclerosis and diabetes result from a host of metabolic abnormalities linked to obesity. Misregulation of homeostatic pathways leads to a constellation of metabolic syndromes, affecting fatty acid and cholesterol metabolism [2]. Regulatory proteins such as PPAR and LXR are targeted for therapeutic study, where an exclusive pharmacological profile is contested. For example, fibrate compounds have been implemented in multiple studies to further characterize the role of PPAR α where it has been shown that PPAR α activation by fibrates has beneficial effects on lipid metabolism [4]. Fibrates target PPAR α , inducing an increase in fatty acid oxidation and glucose sparing in the heart and liver, providing beneficial effects such as decreased lipid accumulation as a result of increased HDL's [4]. However, negative side effects often result in increased triglycerides and weight gain [4]. These negative effects could be attributed to another nuclear receptor such as LXR. As with any pharmacological profile, side effects are a rising issue where a PPAR drug could potentially induce an LXR effect, or visa versa, suggesting unanticipated outcomes resulting in dangerous side effects. The primary goal would be to develop or discover a synthetic ligand that would exclusively target a single homeostatic pathway. Synthetic ligands examined in this study presented novel protein-ligand binding

properties, providing a possible explanation for negative side effects in therapeutic use.

To effectively study synthetic ligands and their application to human use, it is necessary to generate full-length human proteins for all experiments. Prior experiments in the lab demonstrated that truncated and full-length forms of these nuclear receptor proteins behave differently. All full-length proteins were purified using affinity chromatography and evaluated via SDS-PAGE, confirming the presence of the desired protein around 50kDa. The use of full-length human proteins bridges the gap between *in vitro* and *in vivo* assays, allowing generation of data applicable to human diagnosis. While *in vivo* assays are still necessary, data generated *in vitro* can still provide valuable insight into therapeutic medicine, further aiding in understanding of diseases linked to atherosclerosis and diabetes.

Ligand binding becomes increasingly complicated as nuclear receptors, LXR and PPAR, form obligate heterodimers with RXR [16]. More recently, it has been shown that LXR can dimerize with PPAR, presenting a novel heterodimer exhibiting cross talk, where ligands can influence heterodimer choice [16, 29]. Of the compounds evaluated in this project, ciprofibrate and T-0901317 exhibited exclusive binding characteristics for PPAR α and LXR α , respectively. Interestingly, fluorobexarotene, a known RXR agonist, demonstrated promiscuous binding to PPAR α , suggesting that previously assumed ligand binding characteristics are not always predictable. This finding could possibly account for negative side effects seen with many pharmaceutical compounds on the market. Therefore, these three compounds were selected for further study regarding the PPAR α -LXR α heterodimer.

The secondary structure of a given protein ensures proper function and directly affects ligand-binding, linking secondary structure to metabolic function. Typically, ligand binding induces changes in secondary structure, characterizing ligand-regulated nuclear transcription factors such as PPAR, LXR and RXR [5]. Subsequently, alterations to protein secondary structure can significantly alter the functionality of a given protein. Likewise, conformational changes, induced by synthetic ligands, become significant in characterizing protein function, relevant to therapeutic medicine.

This study employed the use of circular dichroism to evaluate the heterodimeric structure of hPPAR α -hLXR α in response to synthetic ligands. In the absence of ligand, it was confirmed that the hPPAR α -hLXR α heterodimer is composed of numerous alpha helices, characterized by the circular dichroic spectra. While all three ligands demonstrated changes in heterodimer conformation, compound T-0901317 induced the most significant changes in the alpha-helical nature of the hPPAR α -hLXR α heterodimer. Understanding how certain ligands affect protein secondary structure can provide enhanced understanding of heterodimeric function in metabolism, and its tandem use in therapeutic medicine.

Since ligand binding can affect protein secondary structure, effectively altering metabolic function, another level of complexity arises where protein-protein interactions could be affected. It is possible that the binding affinity of hPPAR α for hLXR α could be altered in the presence of synthetic ligands, presenting possible repercussions when using pharmaceuticals for therapeutic treatment. It then becomes necessary to evaluate protein-protein interactions in the presence of synthetic ligands

to further understand the intricate nature of this novel heterodimer and its role in cholesterol metabolism. Fluorescence resonance energy transfer was used to determine the effects of synthetic compounds on the hPPAR α -hLXR α heterodimer.

Based on preliminary testing, it was determined that Alexa Fluor dye 488 and 555 would be best suitable for these experiments where AF-488hLXR α was termed the donor and AF-555hPPAR α was termed the acceptor. During energy transfer, a noticeable decrease was seen in donor emission, followed by an increase in acceptor emission, when excited at the proper wavelength. Further evaluation of changes in fluorescence allows a binding curve to be generated, where binding affinities can be assessed. In the absence of ligand, the hPPAR α -hLXR α heterodimer exhibited a K_d value of 8 ± 3 nM. When ligands such as ciprofibrate and T-0901317 were introduced, there was an apparent increase in the K_d value, 11 ± 2 nM and 10 ± 2 nM, respectively. This data would suggest that ciprofibrate and T-0901317 induce protein conformational changes that effectively decrease affinity of hLXR α for hPPAR α . On the other hand, fluorobexarotene appeared to enhance binding affinity of hLXR α for hPPAR α , presenting a K_d value of 5 ± 1 nM. This data presents valuable understanding of how synthetic ligands directly affect protein-protein binding, further linking ligand exclusivity to negative side effects in therapeutic use.

The next step was to evaluate these nuclear receptors *in vivo* by using bimolecular fluorescence complementation (BiFC) and live cell imaging. Initially, stably transfected COS-7 cells were desirable due to genomic plasmid integration. These cells were selected by antibiotic resistance and further analyzed by polymerase chain reaction to ensure complete integration of all three nuclear receptor plasmids.

Isolated cellular DNA was evaluated by electrophoresis, yielding bands at 350, 678 and 312 base pairs, indicating the presence of hLXR α , hRXR α and hPPAR α , respectively. While these results were promising, further fluorescence microscopy experiments, employing the use of stably transfected cells, yielded limited success. Resulting cell images displayed punctuate fluorescence, often in vesicles surrounding the nucleus, however, no nuclear fluorescence was seen. Therefore, transient transfections were used to characterize the effects of synthetic ligands.

Accordingly, after transient transfections with the appropriate BiFC plasmids, nuclear localization was visualized in COS-7 cells via fluorescence microscopy. Unlike the stable transfections, these fluorescent images demonstrated distinct nuclear fluorescence, in accordance with the anticipated heterodimeric outcomes. All fluorescent microscopy images displayed a more intense CFP color than YFP, where this phenomenon could be attributed to several possible reasons. First, it is possible that there are simply fewer binding sites for hLXR α -hPPAR α in the COS-7 cell genome than hPPAR α -hRXR α . Yet this is highly unlikely due to the use of equal plasmid amounts in transfections. Secondly, CFP has a higher quantum yield than YFP, meaning the ratio of photons absorbed to photons emitted is much higher for CFP, resulting in a brighter signal. The later point becomes significant when analyzing subcellular localization since pixel overlap between images can be affected by this phenomenon. Accordingly, the overlap coefficient, R , was used for co-localization quantitation since it is characterized by pixel correlations, insensitive to fluorescence intensity.

To correct for variations seen in fluorescence intensity, images were analyzed by correcting for total cell fluorescence, using measurements of integrated density, area of selected cells and the mean fluorescence of background readings. After total cell fluorescence was corrected, quantitative analysis yielded minimal variations in fluorescence intensity in response to synthetic ligands. Logically, it could be assumed that a ligand, which inhibits or lessens the binding affinity of hPPAR α -hLXR α , would result in a decreased yellow signal. Presumably, such would be the case for ciprofibrate and T-0901317, however, it is possible that the cell's response is to compensate for this "inhibition" by producing more hPPAR α and hLXR α . This phenomenon would effectively mask any effects seen with fluorescence intensity, which could explain the minimal changes in fluorescence intensity. Subsequently, the use of the co-localization overlap, R, becomes necessary for further evaluation.

When the overlap coefficient, R, is plotted against previously determined K_d values from FRET, a small trend emerges. It would seem that co-localization decreases as the K_d value increases. Co-localization, in this case, is evaluating the presence of two heterodimers, hPPAR α -hLXR α and hPPAR α -hRXR α , in the nucleus. The binding affinity values are only for hLXR α -hPPAR α , therefore, synthetic ligands could have unforeseen effects on hRXR α -hPPAR α localization. This is especially plausible since ligand binding was shown to be non-exclusive in the case of fluorobexarotene. This experiment was performed twice, producing similar results in each case (Supplemental Figure 3A and 3B).

If certain ligands affect hLXR α -hPPAR α binding, the cell could attempt to compensate for this effect by making more protein, effectively masking variations in

fluorescence intensity or co-localization. Based on results established from intrinsic fluorescence quenching and FRET assays, we would anticipate seeing some kind of change in fluorescence intensity or co-localization with the addition of a synthetic ligand. The results achieved with BiFC did not produce the desired outcome with synthetic ligands for several variable factors. First, there are distinct differences between proteins evaluated in a cuvette versus a living cell. Secondly, the *in vitro* assays were performed under conditions where the reaction between PPAR α and LXR α was reversible; therefore, the binding affinity (K_d) value was significant. The BiFC experiments required a covalent link between the two proteins of interest (PPAR α and LXR α) due to the nature of the fluorophores. In this case, the resulting reaction between the two proteins was irreversible and the relevancy of binding affinity (K_d) between PPAR α and LXR α in the presence of synthetic ligands becomes questionable. Third, there are distinct differences in the amount of protein utilized during *in vivo* and *in vitro* assays. The CMV promoter used in the experiment is a strong viral promoter and produces high levels of receptors (unlike the native promoters would) and this high level of protein may be too high for this experiment to reveal the differences we anticipated. The high protein levels in a living cell could explain the small changes in co-localization. Alternative methods for regulating protein levels in the cell may allow us to reveal the differences *in vivo* that were observed *in vitro*.

In conclusion, this project has demonstrated novel properties of ligand binding, secondary structures, protein-protein interactions and *in vivo* effects, relevant to the therapeutic treatment of diseases associated with obesity and diabetes.

Understanding how current pharmaceuticals affect nuclear receptors in the human body, can lead to a better platform to assess a host of diseases associated with diabetes. Diseases such as atherosclerosis, hypertriglyceridemia, hypertension and insulin resistance could benefit from this research. Intricate knowledge of cholesterol and fatty acid metabolism can help scientists further develop drugs to accurately balance metabolic homeostasis, potentially minimizing negative side effects for therapeutic application.

VI. LIST OF ABBREVIATIONS

- ABC - ATP binding cassette
- ACOX1 - peroxisomal acyl-coenzyme A oxidase
- Apo – apolipoprotein
- ChREBP - cholesterol regulatory element binding protein
- CYP7A1 - cholesterol 7 α -hydroxylase
- FABP1 - fatty acid binding protein 1
- FAS – fatty acid synthase
- FDA – Federal drug administration
- HDL - high-density lipoprotein
- HMG-CoA - 3-hydroxy-3-methylglutaryl-coenzyme A
- HNF4A – hepatocyte nuclear factor 4 alpha
- IPTG – isopropyl β -D-1-thiogalactopyranoside
- LB – Luria Bertani media
- LBD – ligand binding domain
- LPL - lipoprotein lipase
- LXR – liver X receptor
- N-CoR – nuclear co-repressor
- PMSF – phenylmethylsulfonyl fluoride
- PPAR – peroxisome proliferator-activated receptor

PPRE - peroxisome proliferator response element

RXRE – retinoid X receptor response element

RXR – retinoid X receptor

SMRT – silencing mediator for retinoid and thyroid hormone receptors

SPR – surface plasmon resonance

SREBP-1 - sterol regulatory element-binding protein

TGFB – transforming growth factor beta

UCP – uncoupling protein

VII. REFERENCES

1. Rakhshandehroo, Maryam, et al. "Peroxisome proliferator-activated receptor alpha target genes." *PPAR research* 2010 (2010).
2. Li, Andrew C., and Christopher K. Glass. "PPAR-and LXR-dependent pathways controlling lipid metabolism and the development of atherosclerosis." *Journal of lipid research* 45.12 (2004): 2161-2173.
3. Ide, Tomohiro, et al. "Cross-talk between peroxisome proliferator-activated receptor (PPAR) α and liver X receptor (LXR) in nutritional regulation of fatty acid metabolism. II. LXRs suppress lipid degradation gene promoters through inhibition of PPAR signaling." *Molecular Endocrinology* 17.7 (2003): 1255-1267.
4. Ferré, Pascal. "The biology of peroxisome proliferator-activated receptors relationship with lipid metabolism and insulin sensitivity." *Diabetes* 53.suppl 1 (2004): S43-S50.
5. Hostetler, Heather A., et al. "L-FABP directly interacts with PPAR α in cultured primary hepatocytes." *Journal of lipid research* 50.8 (2009): 1663-1675.
6. Hong, Cynthia, and Peter Tontonoz. "Coordination of inflammation and metabolism by PPAR and LXR nuclear receptors." *Current opinion in genetics & development* 18.5 (2008): 461-467.

7. Desvergne, Béatrice, and Walter Wahli. "Peroxisome proliferator-activated receptors: nuclear control of metabolism 1." *Endocrine reviews* 20.5 (1999): 649-688.
8. Oswal, Dhawal P., et al. "A single amino acid change humanizes long-chain fatty acid binding and activation of mouse peroxisome proliferator-activated receptor α ." *Journal of Molecular Graphics and Modelling* 51 (2014): 27-36.
9. Repa, Joyce J., et al. "Regulation of mouse sterol regulatory element-binding protein-1c gene (SREBP-1c) by oxysterol receptors, LXR α and LXR β ." *Genes & development* 14.22 (2000): 2819-2830.
10. Schultz, Joshua R., et al. "Role of LXRs in control of lipogenesis." *Genes & development* 14.22 (2000): 2831-2838.
11. Zhang, Yuan, et al. "Liver LXR α expression is crucial for whole body cholesterol homeostasis and reverse cholesterol transport in mice." *The Journal of clinical investigation* 122.5 (2012): 1688-1699.
12. Chambon, Pierre. "The retinoid signaling pathway: molecular and genetic analyses." *Seminars in cell biology*. Vol. 5. No. 2. Academic Press, 1994.
13. Kersten, Sander, et al. "Retinoid X receptor alpha forms tetramers in solution." *Proceedings of the National Academy of Sciences* 92.19 (1995): 8645-8649.
14. Mangelsdorf, David J., and Ronald M. Evans. "The RXR heterodimers and orphan receptors." *Cell* 83.6 (1995): 841-850.

15. Balmer, James E., and Rune Blomhoff. "Gene expression regulation by retinoic acid." *Journal of lipid research* 43.11 (2002): 1773-1808.
16. Yoshikawa, Tomohiro, et al. "Cross-talk between peroxisome proliferator-activated receptor (PPAR) α and liver X receptor (LXR) in nutritional regulation of fatty acid metabolism. I. PPARs suppress sterol regulatory element binding protein-1c promoter through inhibition of LXR signaling." *Molecular Endocrinology* 17.7 (2003): 1240-1254.
17. Yue, Liduo, et al. "Ligand-binding regulation of LXR/RXR and LXR/PPAR heterodimerizations: SPR technology-based kinetic analysis correlated with molecular dynamics simulation." *Protein science* 14.3 (2005): 812-822.
18. Ogata, Masaki, et al. "On the mechanism for PPAR agonists to enhance ABCA1 gene expression." *Atherosclerosis* 205.2 (2009): 413-419.
19. Jacobson, Terry A., and Franklin H. Zimmerman. "Fibrates in combination with statins in the management of dyslipidemia." *The Journal of Clinical Hypertension* 8.1 (2006): 35-41.
20. Chiang, John YL, Rhonda Kimmel, and Diane Stroup. "Regulation of cholesterol 7 α -hydroxylase gene (CYP7A1) transcription by the liver orphan receptor (LXR α)." *Gene* 262.1 (2001): 257-265.
21. Xu, Eric H., and Millard H. Lambert. "Structural insights into regulation of nuclear receptors by ligands." *Nuclear receptor signaling* 1 (2003).
22. Duvic, Madeleine, et al. "Bexarotene is effective and safe for treatment of refractory advanced-stage cutaneous T-cell lymphoma: multinational phase II-III trial results." *Journal of Clinical Oncology* 19.9 (2001): 2456-2471.

23. Lalloyer, Fanny, et al. "Retinoid bexarotene modulates triglyceride but not cholesterol metabolism via gene-specific permissivity of the RXR/LXR heterodimer in the liver." *Arteriosclerosis, thrombosis, and vascular biology* 29.10 (2009): 1488-1495.
24. Wagner, Carl E., et al. "Modeling, synthesis and biological evaluation of potential retinoid X receptor (RXR) selective agonists: novel analogues of 4-[1-(3, 5, 5, 8, 8-pentamethyl-5, 6, 7, 8-tetrahydro-2-naphthyl) ethynyl] benzoic acid (bexarotene)." *Journal of medicinal chemistry* 52.19 (2009): 5950-5966.
25. Marconett, Crystal N., et al. "Integrated transcriptomic and epigenomic analysis of primary human lung epithelial cell differentiation." *PLoS genetics* 9.6 (2013): e1003513.
26. Chisholm, Jeffrey W., et al. "The LXR ligand T0901317 induces severe lipogenesis in the db/db diabetic mouse." *Journal of lipid research* 44.11 (2003): 2039-2048.
27. Ding, Xiaobo, et al. "Citrus ichangensis peel extract exhibits anti-metabolic disorder effects by the inhibition of PPAR and LXR signaling in high-fat diet-induced C57BL/6 mouse." *Evidence-Based Complementary and Alternative Medicine* 2012 (2012).
28. Oswal, Dhawal P., et al. "Divergence between human and murine peroxisome proliferator-activated receptor alpha ligand specificities." *Journal of lipid research* 54.9 (2013): 2354-2365.

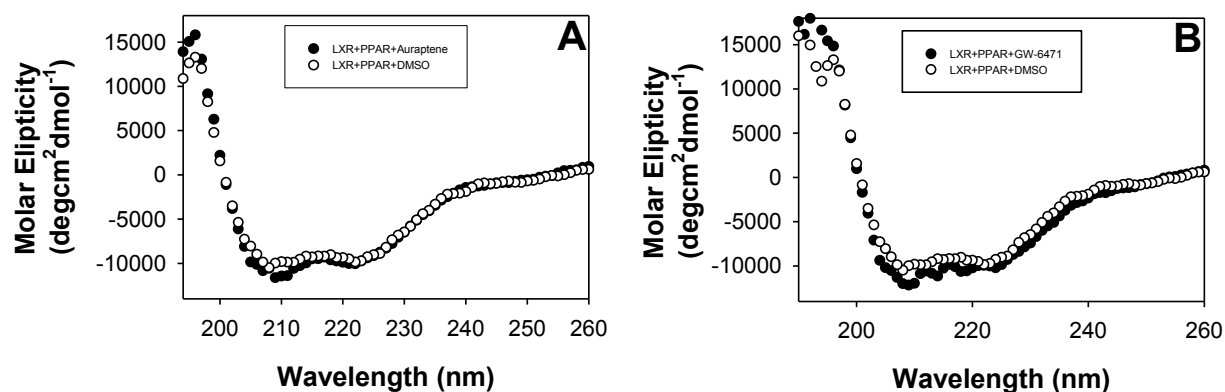
29. Balanarasimha, Madhumitha, et al. "Ligand-Regulated Heterodimerization of Peroxisome Proliferator-Activated Receptor α with Liver X Receptor α ." *Biochemistry* 53.16 (2014): 2632-2643.
30. Kelly, Sharon M., and Nicholas C. Price. "The use of circular dichroism in the investigation of protein structure and function." *Current protein and peptide science* 1.4 (2000): 349-384.
31. Clegg, Robert M. "Fluorescence resonance energy transfer." *Current opinion in biotechnology* 6.1 (1995): 103-110.
32. Shyu, Y. John, et al. "Identification of new fluorescent protein fragments for biomolecular fluorescence complementation analysis under physiological conditions." *Biotechniques* 40.1 (2006): 61.
33. Hu, Chang-Deng, Yurii Chinenov, and Tom K. Kerppola. "Visualization of interactions among bZIP and Rel family proteins in living cells using bimolecular fluorescence complementation." *Molecular cell* 9.4 (2002): 789-798.
34. Hu, Chang-Deng, and Tom K. Kerppola. "Simultaneous visualization of multiple protein interactions in living cells using multicolor fluorescence complementation analysis." *Nature biotechnology* 21.5 (2003): 539-545.

VIII. APPENDIX

Supplemental Table 1. Intrinsic fluorescence quenching of 100nM hLXR α , hPPAR α and hRXR α titrated with synthetic ligands (100 μ M).

Synthetic Compound	K_d (hLXRα) (nM)	K_d (hPPARα) (nM)	K_d (hRXRα) (nM)
Auraptene	ND	5.0 \pm 3.0	ND
GW 6471	7.0 \pm 4.0	67.0 \pm 31.0	ND
Lovastatin	ND	0.6 \pm 0.5	ND
Pravastatin	ND	1.0 \pm 1.0	20.0 \pm 9.0
UVI 3003	ND	ND	10.0 \pm 2.0

ND = Not determinable

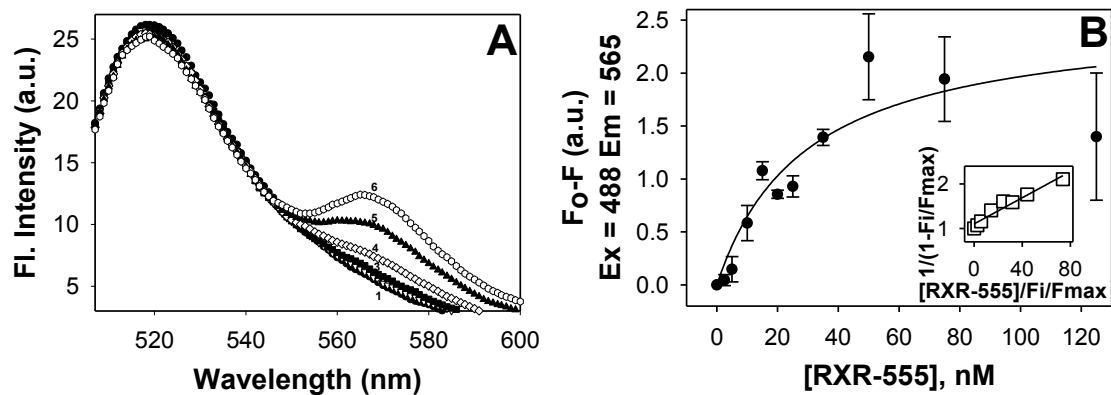


Supplemental Figure 1. Circular Dichroic spectra of a mixture of hPPAR α and hLXR α in the presence and absence of synthetic ligands. (A) Far-UV spectra of a mixture of equal amino acid molarities of hPPAR α and hLXR α in the absence (open circles) and presence (closed circles) of 5 μ M auraptene. (B) Far-UV spectra of a mixture of equal amino acid molarities of hPPAR α and hLXR α in the absence (open circles) and presence (closed circles) of 5 μ M GW-6471. Each spectrum is composed of an average of ten scans, taken from three replicates.

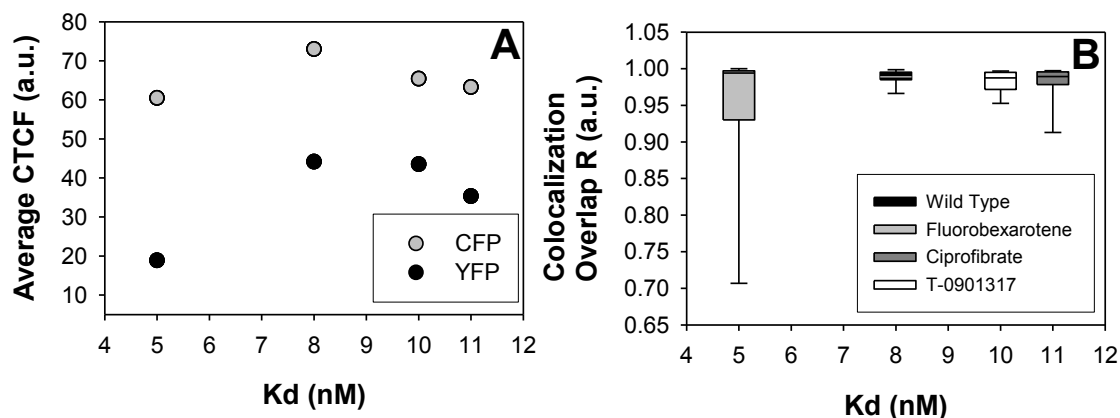
Supplemental Table 2. Secondary structures of hPPAR α and hLXR α (corrected for solvent effect) in the presence and absence of synthetic ligands

Ligand	α -helix	α -helix	β -sheet	β -sheet	Turns	Unrd
	regular	distorted	regular	distorted		
	H(r) %	H(d) %	S(r) %	S(d) %	T %	U %
DMSO	24.5 \pm 0.5	20.5 \pm 3.5	12.0 \pm 2.0	14.5 \pm 0.5	11.5 \pm 0.5	16.5 \pm 0.5
Auraptene	26.3 \pm 0.3	19.3 \pm 1.8	11.3 \pm 1.8	13.7 \pm 0.9	14.0 \pm 2.1	16.3 \pm 0.9
GW 6471	26.3 \pm 1.5	22.7 \pm 1.9	11.3 \pm 1.5	11.7 \pm 1.9	13.7 \pm 0.7	15.0 \pm 0.0

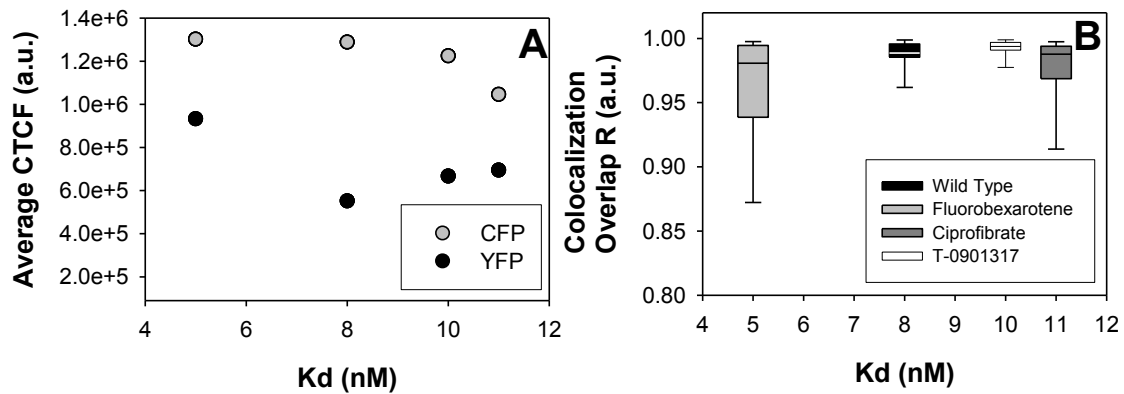
Asterisks (*) represent significant differences due to presence of ligand as compared with the absence of ligand for all panels. *p = <0.06, **p = <0.01, ***p = <0.0001.



Supplemental Figure 2. FRET using AF-488hLXR α as the donor and AF-555hRXR α as the acceptor. (A) 25nM AF-488hLXR α titrated against increasing concentrations of 0nM to 100nM AF-555hRXR α . The x-axis represents wavelength (nm) and the y-axis depicts fluorescence intensity. Excitation wavelength was set at 488nm and emission scans were collected over a range of 500-667nm. (B) 25nM AF-488hLXR α titrated against increasing concentrations of 0nM to 100nM AF-555hRXR α . The x-axis indicates the concentration of AF-555hRXR α and the y-axis represents changes in fluorescence intensity.



Supplemental Figure 3. Quantitative analysis of transiently transfected COS-7 cells in response to synthetic ligands where ECFP-hPPAR α is the central partner receptor. (A) Fluorescence intensity for CFP and YFP in the absence and presence of synthetic ligands. The x-axis indicates K_d values for the hPPAR α -hLXR α heterodimer, previously determined from FRET in the absence and presence of ciprofibrate, fluorobexarotene and T-0901317. The y-axis indicates the average corrected total cell fluorescence (CTCF) for both CFP and YFP. **(B)** Co-localization of hLXR α and hPPAR α in COS-7 cell nuclei in the absence and present of synthetic ligands. The x-axis indicates K_d values for the hPPAR α -hLXR α heterodimer, previously determined from FRET in the absence and presence of ciprofibrate, fluorobexarotene and T-0901317. The y-axis indicates co-localization overlap, R, which is insensitive to variations in fluorescence intensity.



Supplemental Figure 4. Quantitative analysis of transiently transfected COS-7 cells in response to synthetic ligands where ECFP-hLXR α is the central partner receptor. (A) Fluorescence intensity for CFP and YFP in the absence and presence of synthetic ligands. The x-axis indicates K_d values for the hPPAR α -hLXR α heterodimer, previously determined from FRET in the absence and presence of ciprofibrate, fluorobexarotene and T-0901317. The y-axis indicates the average corrected total cell fluorescence (CTCF) for both CFP and YFP. **(B)** Co-localization of hLXR α and hPPAR α in COS-7 cell nuclei in the absence and present of synthetic ligands. The x-axis indicates K_d values for the hPPAR α -hLXR α heterodimer, previously determined from FRET in the absence and presence of ciprofibrate, fluorobexarotene and T-0901317. The y-axis indicates co-localization overlap R, which is insensitive to variations in fluorescence intensity.